Network for the Detection of Stratospheric Change (NDSC) FTIR Intercomparison at Table Mountain Facility, November 1996

A. Goldman
Department of Physics, University of Denver
Denver, Colorado

C. Paton Walsh and W. Bell
National Physical Laboratory, Teddington, England

G.C. Toon, J.-F. Blavier and B. Sen
Jet Propulsion Laboratory, Pasadena, California

M.T. Coffey, J.W. Hannigan and W.G. Mankin
National Center for Atmospheric Research, Boulder, Colorado

Abstract. An intercomparison of four Fourier Transform Infrared (FTIR) spectrometers, operated side by side by JPL, NCAR, and NPL groups, using two different spectral fitting algorithms, was conducted at JPL's Table Mountain Facility (TMF) during November 1996. A "blind" comparison of retrieved vertical column amounts, derived of pre-selected trace gases in pre-selected microwindows (mw), and subsequent re-analysis of the results are described. The species analyzed are N_2 (3 mw), HF (1 mw), HCl (1 mw), CH_4 (1 mw), O_3 (2 mw), N_2O (2 mw), HNO_3 (2 mw), and CO_2 (1 mw). The column agreements from the "blind" phase were within 0.5-2%, except that for HNO_3, HF, and O_3 the range of the results was up to 10%, 5%, and 4% respectively. It was found that several systematic effects were neglected in the "blind" phase analysis. Taking these into account in the post-analysis, reduced the disagreements to 0.5-1.0% for most cases, and to less than 4%, 3% and 1% for HNO_3, HF, and O_3. It was concluded that incomplete knowledge of the instrument response function is the main source of column differences above the 1% level.

1. Introduction

The Network for the Detection of Stratospheric Change [*Kurylo*, 1991] is a set of ground-based observing stations intended to make early detection of changes in the stratosphere, especially changes affecting the ozone layer, and to allow determination of the causes of such changes. Primary and complementary stations are located around the globe, with primary stations, all with the same complement of instruments, located in each of the major latitude zones. The instruments

are carefully calibrated and validated to discern small changes in the stratospheric composition and to help validate global measurements from satellite sensors. Development of the network was started in 1987, began routine operations in 1991, and today is still expanding as new instruments and stations are added. The NDSC is a major component of the international upper atmosphere research effort and has been endorsed by national and international scientific agencies, including the International Ozone Commission, the United Nations Environment Programme (UNEP), and the World Meteorological Organization (WMO).

A formal validation protocol has been adopted to ensure the highest quality measurements, consistent from place to place and over many years [*Kurylo*, 1997]. The Validation Protocol is designed to ensure that the quality of archived NDSC data is as high as possible within the constraints of measurement technology and retrieval theory at the time the data were taken and analyzed. This protocol calls for approval of the design of instruments, testing the data analysis and retrieval methods, initial and periodic "blind" intercomparisons of different instruments of the same type and instruments of different types making measurements of the same quantity, and ongoing tests of the performance of individual instruments. Documentation of instrument characterization, performance, and validation are stored online in the NDSC archives, along with the analyzed data.

The "blind" intercomparisons are an essential component of the evaluation of instrument performance and data analysis. For the blind intercomparisons two or more (as many as possible) instruments are brought together at a common location and observe the natural atmosphere at the same time. Each investigator collects and analyzes his data without any knowledge of the results of other investigators. The data are submitted to an impartial referee, who compares the results from the various instruments participating. The investigators of the instruments being validated agree before the intercomparison to the publication of their results as submitted to the referee. The formal instrument intercomparison can be preceded by a data analysis intercomparison since a full instrument intercomparison is really an intercomparison of the instruments and their associated analysis procedures. In addition, an informal instrument intercomparison can precede the formal one to avert any avoidable problems which could otherwise invalidate the procedures and waste the opportunity. Frequent information comparisons between different instruments and techniques, as well as comparison of analysis and retrieval methods, are encouraged.

Previous NDSC FTIR intercomparisons, each with two Bruker type FTIR spectrometers,

were conducted: (i) During September 24, 1994 -October 14, 1994 at Harestua, Norway (60°N, 10°E), as part of the SESAME project, between National Physical Laboratory (NPL), Teddington, U.K. and Institutet for Vatten-Och Luftvardsforskning (IVL), Göteborg, Sweden; (ii) During May/June 1995 at the arctic station Ny-Ålesund, Spitzbergen (79°N, 12°E), between NPL and Alfred Wegener Institute (AWI), Potsdam, Germany. The results of these two intercomparisons are reviewed and analyzed for vertical column uncertainties in a recent paper by *C. Paton Walsh et al.* [1997].

FTIR spectrometers do not directly measure gas abundances or even spectra. The raw data, the interferograms, are Fourier transformed (after appropriate corrections) to yield the spectrum. The abundances of the various atmospheric gases of interest can then be derived by fitting a synthetic spectrum, calculated line-by-line, to selected intervals of the measured spectra. The software which performs this spectral fitting is commonly termed the retrieval algorithm. A number of retrieval algorithm intercomparisons were conducted by the NDSC IRWG (Infrared Working Group). These include: (i) the ESMOS/NDSC Algorithms Intercomparisons Exercise; Phase 1 was described by *Zander et al.* [1993]. Phase 2 was presented at Brussels April 20-21, 1994, and NCAR, April 26-27, 1995 [*R. Zander*, 1995]. (ii) The NDSC HCl cells intercomparisons, presented at NCAR, April 26-27, 1995 [*A. Goldman et al.*, 1995]; and (iii) the NDSC intercomparison of analysis of ground-based IR synthetic spectra, presented at Garmisch, April 23-25, 1996 [*A. Goldman*, 1996]. However, to date no intercomparisons have been performed of the processing algorithms which transform the raw measured interferograms into spectra.

In contrast to previous FTIR intercomparisons which compared virtually identical instruments and data processing and analysis algorithms, the TMF intercomparison described in this work features a much more diverse set of spectrometers and processing algorithms. Although this diversity makes the intercomparison more challenging, it perhaps provides a better insight into the true accuracy of the measurements.

2. Location and Participants

The FTIR intercomparison was conducted at JPL's Table Mountain Facility (TMF; 34.4°N, 117.7°W) from October 28 to November 15, 1996. This facility is located at an altitude of 2.26 km (typical ground level pressure of 780 mb) in the San Gabriel mountains, which form the northern edge of the Los Angeles basin.

The four participants, their interferometers and spectral fitting codes are listed in Table 1.

Table 1

Short descriptions of instruments used by the groups, their operation during the intercomparison and their approach to the data analysis will be given below.

3. Goals and Method of the Intercomparison

The purpose of this intercomparison was to quantify the level of agreement obtained in vertical column abundances measured by different FTIR spectrometers operated simultaneously and side-by-side, and to investigate the cause of any differences. Under these conditions, the various instruments should obtain essentially the same result, and so any significant discrepancies are indicative of inadequate characterization of the instrument or the retrieval method used to determine the column abundances from the spectra.

It was NOT the purpose of this intercomparison to compare retrieval methods: That can be done with just a computer without the expense of moving instruments to a common site, and several such intercomparisons have been already made [Zander et al., 1993; Zander, 1995]. Therefore, a common approach to the analysis of all the spectra was taken. In particular, consistent assumptions about the state of the atmosphere, the spectroscopic database, and the spectral intervals and gases to be fitted were agreed prior to the intercomparison. This way, any differences that are found in the measured column abundances must be inherent to the spectra themselves, and not to their analysis method.

The intercomparison was divided into two phases: The first week was dedicated to totally open and collaborative work of the groups, to ensure that all measurements and analysis were properly done. The second week was the "blind" comparison, with the agreed conditions as optimized from the first week. The open intercomparison phase clarified problems of instruments,

as well as the adoption of the atmospheric reference profiles and the spectroscopic line parameters before the blind intercomparison started. The "open" days included measurements with an NPL-furnished low pressure HBr cell, inserted in the solar beam, to test the instrument line shape (ILS) of each spectrometer system.

Spectral fittings were for columns only, using the same initial reference gases and pressure-temperature vertical profiles, as prepared by the host (GCT) for typical local conditions. Only scaling of the reference profile was allowed by the fitting. Low sun spectra were avoided, to prevent effects of changing airmass, and hence the need for the measurements to be closely synchronized. The recent intercomparisons conducted at Ny Alesund and Harestua used the same analysis method and a fixed temperature and pressure profile, but used the data from each instrument to converge, independently on a suitable volume mixing ratio (VMR) profile for each day. This allowed independent adjustment of the profiles for best spectral fit, which was forbidden in the present intercomparisons.

The formal results of the "blind" intercomparisons were submitted to a remote referee (A. Goldman) for comparison and evaluation. Subsequently, data were exchanged among the groups. One group (JPL) analyzed data from the four groups and another group (NCAR) analyzed selected data from three groups. The purpose of this effort was to better understand the results, and to separate analysis differences from instrument differences, beyond the scope of the formal intercomparisons. It was anticipated that this phase would enable the identification of systematic effects that were not included previously in the modeling of the instruments. The data were then re-analyzed by each group for a post-intercomparison.

4. Molecules and Microwindows

The spectral regions and species initially selected for fitting are listed in Table 4-1.

Table 4-1

These microwindows are commonly employed by NDSC IR groups for analysis of high priority species. Each window contains relatively strong absorption by the target gases and minimal interference by other absorbers. These regions were pre-agreed by all groups, so that each group would use the same spectral intervals, with the same line parameters.

As shown in Table 1-1, the ATMOS and MkIV groups used the GGG code for spectral fitting, while NCAR and NPL used the SFIT code. In all cases only spectra averaged over pre-determined time interval were analyzed for the vertical column. It was intended that the spectroscopic line parameters be taken from the HITRAN 1992 compilation [*Rothman et al.*, 1992] except for HNO_3 where an updated line list (HITRAN 1996, [*Rothman et al.*, 1998] but without the hotbands) was recommended. It was also decided that for this phase of the intercomparison pressure shifts would not be used in the spectral calculations (even for the CH_4 lines).

Upon completion of their analysis of the "blind" days data, each participant submitted detailed lists of microwindows and species, times of scans and their solar angles, an average column value, and the "uncertainty" of the average. Special conditions during the blind observations have been reported to help in the interpretation of the results, especially when they do not agree.

Note that only one (HNO_3) of the original fitted intervals lies in the HgCdTe region (650-1850 cm^{-1}). As the analysis of the results progressed, it was decided to use additional microwindows for several of the molecules, to be analyzed under the rules of the blind intercomparison. The complete list of the microwindows is given in Table 4-2. The list includes the exact fitting region and molecules that are fitted or fixed (only minute differences among the groups).

Table 4-2

5. The Field Measurements

During the "open" days of the measurements all four interferometers were operated simultaneously, but during the "blind" days, the ATMOS instrument was unable to participate.

During the two days of the "blind" intercomparison there were three measurement periods (Nov. 11A, Nov. 11B, and Nov. 15, 1996). Not all the periods produced the same consistent performance from the interferometers. Each group has evaluated the performance of their instrument and the weather conditions as related to their observed and analyzed results. Observations on 11 November 1996 were made under essentially clear sky conditions. The conditions on 15 November could be described as uniform but thickening cirrus. It has been concluded that Nov. 11B provided the best quality atmospheric conditions and simultaneous instrument performance.

HBr cell spectra were acquired during the open and blind intercomparisons by the MkIV and the two Brukers. The initial analysis showed that all three instruments measured broader HBr line widths than calculated. This led us to conclude (erroneously) that air was leaking into the low pressure HBr cell, causing pressure broadening of the HBr lines, and no further cell spectra were acquired. After the completion of the intercomparison period, it was realized that hyperfine splitting of the HBr lines, not represented in the HITRAN linelist, was actually responsible for the observed broadening [*Coffey et al.*, 1998].

Short JPL (including ATMOS), NCAR and NPL field reports, are given below.

5.1 JPL Report

The MkIV interferometer [*Toon*, 1991] is a FTIR spectrometer built at JPL in 1984. It was designed primarily for use on balloon platforms and performed 11 balloon flights since 1989. It has also made ground-based observations form several sites (including Antarctica in 1986 and Alaska in 1997 and flown on the NASA DC-8 aircraft (polar campaigns; Antarctica in 1987 and the Arctic in 1989 and 1992). ~~This system, as well as ATMOS, have been designated for the NDSC complementary station at TMF.~~

Optically, the MkIV is very similar to the ATMOS instrument, with the main difference that MkIV uses parallel HgCdTe and InSb detectors to cover the entire 650 to 5650 cm^{-1} spectral region simultaneously. The interferometer optics are double passed in order to provide passive shear compensation and a more compact size (1.2x0.7x0.6 m^3), but this limits the maximum usable beam diameter to 30mm (as compared with 60mm for Brukers).

All of the MkIV spectra measured during the blind intercomparison were made with 116 cm OPD. Unlike the Brukers, the MkIV field-of-view diameters (4.3 mrad in HgCdTe and 3.6 mrad in InSb) are defined by apertures deep inside the detector dewars and therefore cannot easily be changed. The broadband operation of the MkIV instrument means that at 116 cm OPD the choice of these field-of-views is optimum only for the center frequency of each detector bandpass. At the high frequency end, the field-of-view limits the MkIV spectral resolution.

The MkIV samples every fringe of a HeNe reference laser, and with a 10kHz sampling rate, takes 3 minutes to record a 116 cm single-sided interferogram. Data are recorded in both the forward and reverse run directions.

During the blind intercomparison, the MkIV took data virtually continuously, with just a few short breaks to check the alignment of the suntracker. The MkIV spectra were subsequently averaged in groups of 4-6 (12-18 minutes) to reduce the labor of analysis, and improve their signal-to-noise ratio. This resulted in 16 average spectra for Nov. 11(day 316) and 3 average spectra for Nov. 15 (day 320). During observations on day 320, made through a thickening layer of cirrus clouds, MkIV saw 50% variations in the InSb zero path difference (ZPD) signal between successive interferograms, whereas under clear sky conditions on day 316 the largest variations were only 1-2%.

Prior to Fourier transformation, the HgCdTe interferograms were corrected for detector non-linearity. In this process, described by *Abrams et al.* [1994], the DC offset is added back onto the AC interferogram, and the result is cubed (the HgCdTe detector is believed to have a response proportional to the cube root of the photon flux). The DC term is then substracted from the interferogram, which is then phase-corrected and Fourier transformed. The resulting spectra typically have zero offsets less than 1%, as compared with 5% if they were not corrected for detector non-linearity.

The ATMOS instrument took data only on Nov. 5 during the open intercomparison. Both the MkIV and ATMOS spectra were analyzed using the GGG software, using 70 layers. The GGG code has been used since 1992 for analysis of MkIV balloon spectra, e.g. *Sen et al.* [1995], and also for analysis of ground-based spectra, e.g. *Notholt et al.* [1997]. It has compared very well with other codes in various algorithm intercomparisons organized on behalf of the NDSC [*Zander et al.*, 1993, 1995; *Goldman*, 1996]. The ATMOS columns abundances were in good agreement with those obtained simultaneously by the MkIV, and the NPL Bruker. During this exercise, all four instruments operated at 50 cm optical path difference in order to match ATMOS, which is unable to operate at higher spectral resolution. The Bruker also took spectra at 117 cm path to match MkIV. Unfortunately, during the week of the blind intercomparison, travel obligations by members of the ATMOS project made them unavailable to run the instrument every day, and on the days when they did come to TMF, the weather was cloudy.

5.2 NCAR Report

NCAR observations were made using a Bruker model 120M spectrometer and separate LN_2-cooled indium antimonide (InSb) or mercury cadmium telluride (HgCdTe) detectors. This system has been designated as one of the NDSC Arctic stations, at Thule, Greenland. Solar radiation was brought into the spectrometer by way of a servo-controlled tracker, which, due to a temporary fault, was manually controlled to limit background fluctuations. Spectra were recorded in each of four infrared bandpass filters covering 3995-4265 cm^{-1} (HF), 2420-3150 cm^{-1} (HCl, O_3, CH_4), 2040-2590 cm^{-1} (N_2O, N_2) and 750-1365 cm^{-1} (HNO_3, CO_2), in approximately 20 minute periods, one devoted to each filter. This was done for each filter on the morning and afternoon of 11 November 1996 and on the morning of 15 November 1996. The FOV values, in order of the above filters list, were 2.96 mrad, 2.96 mrad, 3.86 mrad and 6.36 mrad. All the spectra were taken at 180 cm OPD, except in the HF filter where 128 cm was used.

During the morning session of 11 November 1996 some unusual vibration was observed in the motion of the moving mirror of the Bruker interferometer. An attempt was made to eliminate this vibration by lubricating the slide of the mirror drive after the first two filter sets (filters 6 and 3) of the morning session of 11 November. There appeared to be a significant improvement in signal to noise and in zero level stability after lubricating the slide. It was also observed that vibration of the mirror was reduced at higher scanner velocity so the afternoon session of 11 November and the

15 November session were recorded at the maximum scan speed of 5.06 cm/s, compared to 2.53 cm/s used in the 11 Nov morning session.

The spectral data were analyzed using the line-by-line non-linear least-squares spectral fitting SFIT code [*Rinsland et al.,* 1982] version 1.09, with 41 layers, adapted for the OS/2® operating system. This code is now being used by numerous groups (see, for example, *Zander et al.*, 1995).

5.3 NPL Report

NPL observations were made using a Bruker IFS 120M high resolution Fourier-transform spectrometer and an active solar tracker. This system has been serving as the NDSC mobile interferometer for field intercomparisons and campaigns since 1994. The spectrometer was configured with a CaF_2 beamsplitter and an InSb detector for column measurements of HCl, O_3, CH_4, N_2, N_2O and HF, and with a KBr beamsplitter and a HgCdTe detector for column measurements of HNO_3 and CO_2. NPL used the same narrow band-pass optical filters as NCAR except for the HNO_3 and CO_2 region, where a narrower band-pass of 750-1000 cm^{-1} was used. Most spectra were obtained in 73 seconds with a maximum optical path difference (OPD) of 180 cm (except for spectra in the HF region which took 53 seconds for an OPD of 128 cm).

Spectra were recorded in both forward and backward direction of the mirror traverse, and digital filtering was applied. The nominal aperture settings (and corresponding angular diameter field of view values) were 1.4 mm (6.36 mrad) for HNO_3 and CO_2 ; 0.65 mm (2.95 mrad) or 0.85 mm (3.86 mrad) for N_2 and N_2O; and 0.65 mm for all the other molecules. The instrument performance was consistent throughout the "open" and "blind" measurements.

Vertical column abundances were obtained by spectral fitting each of the individual single scans to an atmospheric model using the SFIT version 1.06 nonlinear least-squares fitting algorithm using 36 layers. A fixed boxcar apodization function was used for all molecules.

On the 5th November 1996, during the "open" phase of the intercomparison, a full set of spectra was recorded at an OPD of 50 cm, simultaneously with ATMOS, MkIV and NCAR. All other conditions were unchanged except that the HNO_3 and CO_2 were measured using an aperture of 1.85 mm (8.41 mrads). A set of HNO_3 measurements was then made at an OPD of 116 cm,

simultaneously with MkIV and NCAR. Deteriorating weather conditions prevented further spectra from being recorded.

6. Column Values and Sample Spectra from the Blind Results

The complete set of results from the three periods of blind intercomparisons is displayed in Tables 6-1 to 6-3. These include individual reports for November 11A, November 11B, and November 15, 1996, complete with times, geometry, number of observations, mean vertical columns and uncertainties. Inspection of these tables shows that in most cases the column agreements are within 1-2%, and some are less than 1%. In particular, the range of agreement for N_2(2418 cm^{-1}), N_2O(2442 cm^{-1}, 2482 cm^{-1}), and CH_4(2904 cm^{-1}) is 0.5-1%. A significant exception is the HNO_3, for which there is >10% range of the results among the groups (not in all data sets). Disagreement ranges of ~5% in HF and ~4% in O_3 are also evident. More detailed discussion and partial resolution of these discrepancies will follow.

Tables 6-1 to 6-3

Sample spectra from the participants, submitted as computer files of observed and fitted, were plotted for each molecule and shown in Figures 1-7. The samples were required to come from similar, but not identical, observation conditions. A summary of the samples for the plots is given in Table 6-4.

Figs. 1-7

Table 6-4

The sample spectra were chosen by each group as "typical". The spectra shown in Figures 1-7 are from approximately 20 minutes of observation. In the case of the Bruker measurements, scans are recorded in both forward and backward traverses of the mirror. A single forward or backward scan, which typically takes just over one minute to record, comprises an individual observation. About 10 spectra are coadded for the 20 minute averages shown in Figures 1-7. In the case of the MkIV, six single scans are coadded over 19 minutes into an individual observation.

The number of individual observations and the uncertainty values as submitted by the participants are included in the summary tables. It should be noted that while each group defines an individual observation in a different way, the theoretical signal to noise improvements obtained over similar observing time intervals should be similar.

For the Brukers, the columns from the individual observations were averaged to yield the reported mean column values. The standard deviation values were taken as the uncertainties. In the MkIV case, the uncertainties are derived from the covariance matrix of the fitted parameters. This results in uncertainties which are proportional to the rms fit over the interval and inversely proportional to the depth and number of target absorption features. Experience has shown that for truly random residual this technique gives uncertainties which are consistent with the statistical scatter of column values. However, when the residuals are dominated by systematic features, consistent from spectrum to spectrum, the uncertainties are more pessimistic than those that would be obtained by statistical analysis of the column values.

In subsequent analysis, it was established (NCAR and NPL group) that the column values obtained from a coadded spectrum of all the individual spectra agree well with the average value of the columns derived from each of the individual spectra. In NCAR's case, the agreement between the two methods was less than 0.5% for all gases except HNO_3, where the agreement was -1.1% and +0.7% for Nov. 11A and Nov. 11B respectively. In NPL's case, the worst agreement was for Nov. 11B, HNO_3, with a 0.14% difference. Thus, the different approaches applied for deriving the average column values are not expected to dominate the differences seen in the summary tables.

In the initial plots of these samples, it was found that the wavenumber scale differs from one group to another and a small correction was needed (of the order of 0.004 cm^{-1}). While such shifts are removed in the spectral fitting procedure, it will be beneficial that each group maintain exact wavelength calibration. Note that the microwindows and the fitted or fixed molecules are similar, but not always identical, among the groups (see Figs. 1-7 and Table 4-2; some of the microwindows differ by ~0.02 cm^{-1}). The plots have been expanded vertically to better show the fitting.

Figs. 8,9

In some cases the fittings show that the peak absorption of a main line of interest is consistently under(over) calculated, or slightly asymmetrical due to pressure shifts. Typical examples are N_2O and CH_4 (see Figures 8 and 9). As was shown by a number of published and unpublished studies of N_2O (e.g. *Zander et al.*, [1994]), this could be corrected by a vertical shift of the reference profile. Indeed, results from spectral fitting in the N_2O region (2480 cm^{-1}) from each of the instrument teams show residuals similar to that in the top panel of Figure 8. A second

fit to the spectra in Figure 8 was performed using an N_2O mixing ratio profile which was shifted upward by about 5 km. The observed and calculated spectra and residual from the second fitting is shown in the bottom panel of Figure 8. The improvement is obvious. However, it was chosen not to shift the profile, only for the purpose of maintaining consistency in the intercomparison.

In the case of CH_4, the initial JPL sample spectrum included pressure shift in the spectral calculations, while the samples from the other two groups were fitted without it. As is well known, including the pressure shift improves the spectral fit and increases slightly the column amount. The CH_4 pressure shift was not included in the post-intercomparison analysis.

An attempt was made at the beginning of the intercomparison to choose mixing ratio profiles for all the target and contributing gases which were appropriate to the conditions of the observing period. This was not fully achieved for the case of N_2O. However, the objective of the intercomparison was not to retrieve the best possible VMR profiles for the days of observation but rather to compare instruments and retrieval techniques with similar inputs. Results from the various groups have not been revised to account for improved knowledge of the VMR distributions although this will be an important area of concern when the instruments begin observations from their respective NDSC sites.

7. Initial Analysis of the Discrepancies in HNO_3, HF, and O_3

The HNO_3 column results show discrepancies in the range of 11% on Nov. 11A, and Nov. 15 (both larger than the quoted uncertainty), but only 7% on Nov. 11B (still outside the quoted uncertainty). The HF discrepancy ranges are 5% for both Nov. 11A and Nov. 11B, and 4% for Nov. 15, all outside the range of the uncertainty. For O_3, 4% on Nov. 11A and Nov. 11B (within the range of uncertainties), and 5% on Nov. 15 (outside the range of the uncertainty).

Direct examination of the spectra from the cases of large HNO_3 column discrepancies does not reveal obvious deficiencies compared to other spectra that yielded compatible columns. In an effort to better understand the sources of the discrepancies, the groups conducted an extensive investigation of their own spectra as well as of each others' spectra (which were exchanged after the "blind" results of all the microwindows were submitted to the referee). The initial studies have dealt with a number of issues, important not only to this particular intercomparison, but to other

NDSC investigations and atmospheric spectroscopy in general.

The major issues were the implementation of zero level offset, the channel spectrum correction, and modeling of the instrument function. All three instruments exhibit the well known zero level offsets in the HgCdTe region, of 3 to 6%. The JPL spectra include a zero level correction, while those by NCAR and NPL do not. For a weak (linear) absorption, such as in the case of HNO_3, a 5% positive zero offset corresponds to a ≈5% increase in the derived column amount. For stronger absorption as in the CO_2 case, from a 2% zero offset, ≈3% column increase is expected. It was recognised that such corrections will eliminate a large portion of the disagreements for HNO_3 and CO_2.

In the case of HF, it appears that the incomplete modeling of the instrument function is responsible for a major part of the consistent discrepancies among the instruments. See also section 8.

The discrepancies in the O_3 results are not consistent among the microwindows during the "blind" days. The 11B results in the 3045 cm^{-1} microwindow are within 1%, which may indicate that no serious misinterpretation occurred in the analysis.

8. Post-Analysis of the Intercomparison

Subsequent to the initial analysis of the blind intercomparison (section 7), and following a number of group discussions, it was recognized that post-analysis of the same data will be valuable for extracting the most information from the measurements and validating the quality of the results. The conclusions of the re-analysis by each group are given below. The major correction found to be needed is for the zero offsets in the HgCdTe region of the Brukers (and ATMOS) spectra (see Tables 8-1, 8-2). The newly derived columns are shown in Tables 8-3 to 8-5.

8.1 JPL Post-analysis

Compared to the originally submitted MkIV results, the following changes in the analysis were made:

1) The real altitude of TMF (2258m) has been used instead of the pressure altitude (the altitude in the chosen T/P model corresponding to the measured surface pressure).

2) The HNO_3 "hot bands" around 870 cm^{-1} have been removed from the linelist, and only the main bands updated set has been used (see section 4).

3) An improved algorithm for fitting the channel fringes has been used. The original algorithm required that the user first determine the period of the channel fringes (which is usually almost constant for a given set of runs) and then the algorithm would determine their amplitude and phase for each spectrum. The new algorithm fits their amplitude period and phase automatically.

4) The algorithm for determining the uncertainty in the retrieved vertical column abundances has been improved by a more realistic treatment of the effects of uncertainties in the zero level of the spectra. Thus, although this change does not alter the column abundances themselves, their error bars will be slightly different.

Note that no intensity offsets were used in the analysis of the MkIV spectra. However, since ATMOS uses its HgCdTe detector in all spectral regions, and since the detector non-linearity correction described by *Abrams et al.* [1994] only works for ATMOS filters 1 and 2, empirical offsets were adopted for ATMOS filters 3 and 4.

The results of the post-analysis of the JPL data show only small changes, of less than ~0.5%, for most molecules. The exception is HNO_3 for which the new column values are lower by up to 3%, due to both the new channel fringe fitting (2%) and the rejection of the HNO_3 hot

band lines (1%).

8.2 NCAR Post-analysis

After the initial, blind analysis of NCAR spectra to produce results, which are contained in Tables 6-1 to 6-3, it was recognized that improvements could be made in the fitting procedures. Two particular features of the analysis were examined.

A HgCdTe detector was used for spectra recorded at the longest wavelengths (Filter 6) which included features of HNO_3 and CO_2. These spectra exhibit a zero level offset, presumably due to the response of the detector. The zero level offset, which was in the range of 2 to 6% above zero, was not accounted for in the blind phase of the analysis. Offsets were determined by increasing the width of the spectral region near the target lines of HNO_3 and CO_2 until fully absorbing lines of some gas are encountered on each side of the region of interest. A straight line connecting the depths of these fully absorbed lines was found to be parallel to the initial zero level and was adopted as the zero offset. The magnitudes of the offsets are different for the three observing periods and spectral regions and are shown in Table 8-1. For the relatively weak absorption by HNO_3 and CO_2 in these measurements, the effect of an upward shift in zero level is to increase the retrieved column amount by approximately the same percentage as the offset. Results accounting for the zero level offset are contained in Table 8-1.

Table 8-1

A second feature of the analysis which was found to be less than optimum was the number of iterations allowed in the spectral least squares fitting routine, SFIT. For all the cases submitted in the blind intercomparison phase the maximum number of iterations was unnecessarily set to 5. For some spectral regions this limit did not allow the best fits to be achieved. A re-analysis of all spectra was performed with the maximum iterations set to 20. For O_3 fits near 3045 cm^{-1} allowing 6-9 iterations in SFIT, rather than the previous limit of 5, increased the retrieved columns by about 3% and considerably reduced the deviations of the fits. For HNO_3 fits near 873 cm^{-1} 6 to 8 iterations, rather than 5, reduced the retrieved columns by about 4% but did not significantly change the standard deviations. For all other gases and fit regions, allowing iterations up to 20 did not change the retrieved column by more than 1%.

8.3 NPL Post-analysis

All of the spectra taken using the HgCdTe detector were reanalysed in an attempt to compensate for the effects of non-linearities. For the HNO_3 fitting, SFIT was used to fix the base-level at a value closest to where the nearby H_2O absorption saturates. The level at which this H_2O line saturates was termed the zero level. Shifting the assumed zero to this value has the effect of increasing the derived HNO_3 column by an equivalent percentage, e.g. spectra in Set 1 had a mean zero level of 0.039 which resulted in an approximate increase of 3.9% in the resulting derived mean column. It should be noted that this is an approximate non-linearity correction which neglects any possible contribution to the offset from emission. This approximation has been made in order that we may establish if non-linearity is the main cause of discrepancies between the HNO_3 columns reported by different groups.

For the CO_2 fitting a similar approach was attempted. The zero offset in the NPL spectra is not constant at all frequencies so the decision as to where to set the zero was somewhat arbitrary. For example a typical spectrum from the 11th November gives a zero offset of 4% at 871.2 cm^{-1} and 2.6% at 909.2 cm^{-1}. Since there were no saturated absorptions recorded to the other side of the CO_2 feature the zero level at 909.2 cm^{-1} line was used and then adjusted for the change in continuum level near the CO_2 absorption. This approach was used for the purposes of trying to understand the cause of differences between the reported CO_2 columns and gave zero offset values and "corrected" columns. The results for both HNO_3 and CO_2 are given in Table 8-2.

Table 8-2

Table 8-3

Table 8-4

Table 8-5

8.4 Multi-Group Re-Analysis

To separate potential differences due to the analysis methods from the instrumental effects, two groups re-analyzed data from all the groups using two codes. As part of this analysis, both codes, GGG and SFIT, were applied to the data from all three groups. The JPL group analyzed all the data available during both the open and blind intercomparison periods from JPL, NCAR, NPL and ATMOS with the GGG code, and the NCAR group analyzed selected data sets from JPL, NCAR and NPL data with the SFIT code.

Figs. 10-13

Figs. 10-13 show samples from the JPL-GGG analysis of all the available data for the HNO_3 868 cm^{-1}, HCl 2925 cm^{-1}, O_3 3045 cm^{-1}, and HF 4039 cm^{-1} microwindows. The Nov. 5 open intercomparison data of ATMOS, MkIV and NPL Bruker are included in these Figures (data from NCAR Bruker were not available from that day). Figs. 14-17 show the corresponding NCAR-SFIT analysis for the periods of the simultaneous group measurements, which also include the results from the two codes as applied to the same data sets.

confirmed w/ not previous algorithm intercomparisons but showed:

Figs. 14-17

The results ~~show~~ that the differences in column values between the codes are not a major source of the disagreements in the open and blind intercomparisons. It was uniformly concluded that the major corrections needed were the intensity offsets in the HgCdTe region. The selection of the HCl microwindow from the InSb range eliminated the sensitivity to the different ways the two codes correct for zero level and channel spectra. The HF microwindow demonstrates larger instrument alignment sensitivity than the longer wavelength microwindows.

Re-analysis of the HBr cell spectra revealed certain deficiencies in modeling the instrument functions. Spectral simulations showed that, in principle, correction factors could have been derived if more systematic spectra of the HBr cell were available. The LINEFIT procedure [*Hase et al.*, 1999] is applicable for this purpose.

9. Comparisons with ATMOS Data

As mentioned above, ATMOS data were available only during the "open" intercomparison period. These data are not sufficient for NDSC instrument validation, but do provide important comparisons with the JPL, MkIV and NPL Bruker data ....

• • •

10. Conclusions

Several conclusions can be drawn from the results of this intercomparison campaign which are relevant for the general validation methods of FTIR measurements in the NDSC, and specifically confirm that the instruments involved in this intercomparison met the NDSC validation requirements.

The most significant conclusion for the operation of the NDSC is that the differences between performance of any of the instruments and their associated data analysis need not be an

important factor in the accuracy of the results of NDSC observations with these instruments. All instruments performed very well during the selected days. Other factors introducing common errors (e.g. spectroscopic parameters) or error specific to observations (e.g. vmr profile shapes) will be substantially larger than differences which can be attributed to a particular instrument. The differences between the results of the blind intercomparisons run about 1-2% except in the cases of HNO_3 and HF. The subsequent reanalysis, based on a known zero level problem of the Brukers in the HgCdTe region, which was not included in the analysis in the blind intercomparison phase, for HNO_3 (the only gas initially retrieved in the HgCdTe region) significantly reduced the differences from around 5% to around 3%. In the case of HF where the short wavelength exacerbates any instrument alignment problems, the reanalysis did not resolve the discrepancies of around 3%. Small instrumental effects which are not understood remain; they are probably related to the incomplete determination of the instrument line shape. In actual observations, however, where the instruments are located at sites far from each other and at widely different latitudes (and hence solar elevation angles), differences in the zenith angles, atmospheric temperatures, and in the assumed shapes of the vmr profiles (both target and interfering gases) are likely to produce errors substantially larger than those produced by differences in the instruments observing under identical conditions with common assumptions.

The tests in which data from one instrument were analyzed using the analysis techniques of the team from another instrument produced results generally within about 1% of the values produced by the instrument team using its preferred analysis method. This confirms results from previous intercomparisons [*Zander et al.*, 1993; *Zander,* 1995; *Paton Walsh et al.*, 1997] of analysis methods in cases using common spectra and closely matched atmospheric and spectral parameters. It can therefore be concluded that there will be little if any systematic bias in results depending upon the analysis method.

To obtain the precision determined in this intercomparison, the instruments must be adjusted very nearly to their optimum conditions and operated and maintained in that condition. Small departures from optimum alignment or operation (such as the velocity variations introduced by the lubrication problems in the NCAR Bruker during observing period Nov. 11A) can have a detrimental effect on instrument line shape, phase corrections, and noise, resulting in poorer accuracy and precision. Excess noise is easy to recognize by comparison with previous observations; errors in the ILS are more difficult to diagnose, but can frequently be recognized in spectra of narrow spectral lines in a cell at known pressure and temperature; phase errors can

manifest themselves as asymmetries in the shape of intrinsically symmetric lines or in slopes of the bottoms of saturated lines.

Finally, we make some observations on the intercomparison campaign itself. Campaigns that bring large, complex instruments together at a common location are difficult and costly. Although it may be desirable to separate, or extend the time interval between, the open and blind intercomparisons until all major difficulties and differences are resolved, cost constraints and scheduling problems argue against this. We believe that the method we have used, an open intercomparison in which we try to learn optimal methods and correct any problems, followed immediately by a blind intercomparison in which data are collected at the same time and under the same conditions, but analyzed without any communication between groups, followed by a post-analysis and comparison of methods to determine the cause of any discrepancies, is an excellent mechanism for both optimizing the instruments' performance and verifying the accuracy to which they agree. The reanalysis after the blind intercomparison and the analysis of each group's data by other groups was valuable because it captured what we learned from the intercomparison, eliminated errors, and produced the best answers.

Acknowledgments. The work at both the University of Denver and at the National Center for Atmospheric Research (NCAR) was supported in part by the National Science Foundation and in part by the NASA Upper Atmosphere Research Program. The authors would like to thank the UK Department of Environment, Transport and the Regions for support of this work. Part of this work was performed at the Jet Propulsion Laboratory, California Institute of Technology, under contract with NASA. We wish to thank Dan Sidwell, Pam Glatfelter, Stuart McDermid, Dan Walsh, Dave Petterson, and other TMF personnel who supported this intercomparison.

References

Abrams, M.C., G.C. Toon, and R.A. Schindler, Practical example of the correction of Fourier transform spectra for detector non linearity, *Appl. Opt.*, 33, 6307-6314, 1994.

Coffey, M.T., A. Goldman, J.W. Hannigan, W.G. Mankin, W.G. Schoenfeld, and C.P. Rinsland, Improved vibration-rotation (0-1) HBr line parameters for validating high resolution infrared atmospheric spectra measurements, *J. Quant. Spectrosc. Radiat. Transfer*, 60, 863-867, 1998.

Goldman, A., Status of HCl cell intercomparison, NDSC Infrared Working Group Meeting, NCAR Mesa Lab, April 26-27, 1995, Boulder, CO.

Goldman, A., Intercomparison of analysis of ground-based IR synthetic spectra, NDSC Infrared Working Group Meeting, Garmisch, Germany, April 23-25, 1996.

Hase, F., T. Blumenstock, and C. Paton Walsh, Analysis of instrumental line shape of high-resolution FTIR-spectrometers using gas cells measurements and a new retrieval software, *Appl. Opt.*, in press, 1999.

Kurylo, M.J., Network for the detection of stratospheric change (NDSC). Proceedings of SPIE The International Society for Optical Engineering, Remote Sensing of Atmospheric Chemistry, 1991, 1491, 168-174.

Kurylo, M.J., Network for the Detection of Stratospheric Change (NDSC): Validation Protocol; Appendix IV: Infrared Instruments (FTIR), http://climon.wwb.noaa.gov.

Notholt, J., G.C. Toon, R. Lehmann, B. Sen, and J.-F. Blavier, Comparison of Arctic and Antarctic trace column abundances from ground-based Fourier transform infrared spectroscopy, *J. Geophys. Res.*, 102, 12863-12869, 1997.

Paton Walsh, C., W. Bell, T. Gardiner, N. Swann, P. Woods, J. Notholt, H. Schutt, B. Galle, W. Arlander, and J. Mellqvist, An uncertainty budget for ground-based FTIR column measurements of HCl, HF, N_2O and HNO_3 deduced from results of side-by-side instrument intercomparisons, *J. Geophys. Res.*, 102, 8867-8873, 1997.

Rinsland, C.P., M.A.H. Smith, P.L. Rinsland, A. Goldman, J.W. Brault, and G.M. Stokes, Ground-based infrared spectroscopic measurements of atmospheric hydrogen cyanide, *J. Geophys. Res.*, 87, 11119-11125, 1982.

Rothman, L.S., R.R. Gamache, R.H. Tipping, C.P. Rinsland, M.A.H. Smith, D.C. Benner, V. Malathy Devi, J.-M. Flaud, C. Camy-Peyret, A. Perrin, A. Goldman, S.T. Massie, L.R. Brown, and R.A. Toth, The HITRAN molecular database: Editions of 1991 and 1992, *J. Quant. Spectrosc. Radiat. Transfer*, 48, 469-507, 1992.

Rothman, L.S., C.P. Rinsland, A. Goldman, S.T. Massie, D.P. Edwards, J.-M. Flaud, A. Perrin, C. Camy-Peyret, V. Dana, J.-Y. Mandin, J. Schroeder, A. McCann, R.R. Gamache, R.B. Watson, K. Yoshino, K. Chance, K. Jucks, L.R. Brown, V. Nemtchinov, and P. Varanasi, The HITRAN Molecular Spectroscopic Database and HAWKS (HITRAN Atmospheric Workstation), *J. Quant. Spectrosc. Radiat. Transfer*, 60, 665-710, 1998.

Sen, B., G.C. Toon, J.-F. Blavier, J.T. Szeto, E.L. Fleming, and C.H. Jackman, Balloon-borne observations of mid-latitude hydrofluoric acid, *Geophys. Res. Lett.*, 22, 835-838, 1995.

Toon, G.C., The JPL MkIV Interferometer, *Optics and Photonics News*, 2, 19-21, 1991.

Zander, R., Ph. Demoulin, E. Mahieu, G.P. Adrian, C.P. Rinsland, and A. Goldman, ESMOSII/NDSC IR spectral fitting algorithms intercomparison exercise, Proceedings of the Atmospheric Spectroscopy Applications Workshop, University of Reims Champaigne Ardenne, France, Eds. A. Barbe and L. Rothman, September 8-10, 1993.

Zander, R., D. H. Ehhalt, C. P. Rinsland, U. Schmidt, E. Mahieu, J. Rudolph, P. Demoulin, G. Roland, L. Delbouille, and A. J. Sauval, Secular trend and seasonal variability of the column abundance of N_2O above the Jungfraujoch station determined from solar spectra, *J. Geophys. Res.*, 99, 16,745-16,756, 1994.

Zander, R., IR retrieval algorithms intercomparison for the NDSC, Fourier Transform Spectroscopy: New Methods and Applications, Opt. Soc. Conference, Feb. 9-11, 1995, Santa Fe, New Mexico.

A. Goldman, Department of Physics, University of Denver, Denver, CO 80208, USA (e-mail: agoldman@du.edu)

C. Paton Walsh and W. Bell, National Physical Laboratory, Queens Road, Teddington, Middx. TW11 OLW, England (e-mail: clare.paton-walsh@npl.co.uk; wb@newton.npl.co.uk)

G. C. Toon, B. Sen and J.-F. Blavier, Jet Propulsion Laboratory, California Institute of Technology, Pasadena, CA 91109, USA (email: toon@mark4sun.jpl.nasa.gov; blavier@mark4sun.jpl.nasa.gov; bhaswar@mark4sun.jpl.nasa.gov)

M. T. Coffey, J. W. Hannigan, and W. G. Mankin, Atmospheric Chemistry Division, National Center for Atmospheric Research, Boulder, CO 80307, USA (e-mail: coffey@ncar.ucar.edu; jamesw@ncar.ucar.edu; mankin@ncar.ucar.edu)

Legend for Tables

Table 2-1. Groups and Instruments Participating in the NDSC TMF Intercomparisons, Nov. 1996

Table 4-1. Initial Microwindows for the Blind Intercomparison, NDSC TMF, Nov. 1996

Table 4-2. Microwindows and Species used for the Blind Intercomparison, NDSC TMF, Nov. 1996

Table 6-1. Summary of Column Measurements from the Blind Intercomparison, NDSC TMF, Nov. 11, 1996A

Table 6-2. Summary of Column Measurements from the Blind Intercomparison, NDSC TMF, Nov. 11, 1996B

Table 6-3. Summary of Column Measurements from the Blind Intercomparison, NDSC TMF, Nov. 15, 1996

Table 6-4. Summary of the Column Measurements of Coadded Spectra from the Blind Intercomparison as used for the Spectral Plots in Figs. 1-7

Table 8-1. Zero Level Corrections for HNO_3 and CO_2 Analysis, NCAR Post-Analysis

Table 8-2. Zero Level Corrections for HNO_3 and CO_2 Analysis, NPL Post-Analysis

Table 8-3. Summary of Column Measurements from the Post-Analysis, NDSC TMF, Nov. 11, 1996A

Table 8-4. Summary of Column Measurements from the Post-Analysis, NDSC TMF, Nov. 11, 1996B

Table 8-5. Summary of Column Measurements from the Post-Analysis, NDSC TMF, Nov. 15, 1996

Legend for Figures

Figure 1. Solar spectra (observed and calculated) obtained by the JPL, NCAR and NPL groups in the HNO_3 868 cm^{-1} microwindow. See Table 6-4 for details.

Figure 2. Solar spectra (observed and calculated) obtained by the JPL, NCAR and NPL groups in the N_2 2418.6 cm^{-1} microwindow. See Table 6-4 for details.

Figure 3. Solar spectra (observed and calculated) obtained by the JPL, NCAR and NPL groups in the N_2O 2481.3 cm^{-1} microwindow. See Table 6-4 for details.

Figure 4. Solar spectra (observed and calculated) obtained by the JPL, NCAR and NPL groups in the CH_4 2903.8 cm^{-1} microwindow. See Table 6-4 for details.

Figure 5. Solar spectra (observed and calculated) obtained by the JPL, NCAR and NPL groups in the HCl 2925.9 cm^{-1} microwindow. See Table 6-4 for details.

Figure 6. Solar spectra (observed and calculated) obtained by the JPL, NCAR and NPL groups in the O_3 3045.2 cm^{-1} microwindow. See Table 6-4 for details.

Figure 7. Solar spectra (observed and calculated) obtained by the JPL, NCAR and NPL groups in the HF 4038.9 cm^{-1} microwindow. See Table 6-4 for details.

Figure 8. Spectral least squares fitting (NCAR, with the SFIT code) to solar spectra in the N_2O 2481.3 cm^{-1} microwindow for "standard" and shifted N_2O vertical profiles.

Figure 9. Spectral least squares fitting (JPL, with the GGG code) to solar spectra in the CH_4 2903.8 cm^{-1} microwindow, with and without pressure-shift.

Figure 10. Column results by JPL GGG analysis during Nov. 5, 1996, Nov. 11, 1996 and Nov. 15, 1996 in the HNO_3 868 cm^{-1} microwindow, including all available data from JPL (MkIV (•) and ATMOS (◊)), NCAR (∇) and NPL (□).

Figure 11. Column results by JPL GGG analysis during Nov. 5, 1996, Nov. 11, 1996 and Nov. 15, 1996 in the HCl 2925.9 cm^{-1} microwindow, including all available data from JPL (MkIV (•) and ATMOS (◊)), NCAR (∇) and NPL (□).

Figure 12. Column results by JPL GGG analysis during Nov. 5, 1996, Nov. 11, 1996 and Nov. 15, 1996 in the O_3 3045.2 cm^{-1} microwindow, including all available data from JPL (MkIV (•) and ATMOS (◊)), NCAR (∇) and NPL (□).

Figure 13. Column results by JPL GGG analysis during Nov. 5, 1996, Nov. 11, 1996 and Nov. 15, 1996 in the HF 4039 cm^{-1} microwindow, including all available data from JPL (MkIV (•) and ATMOS (◊)), NCAR (∇) and NPL (□).

Figure 14. Column results from NCAR SFIT analysis and JPL GGG analysis of spectra from JPL, NCAR and NPL in the HNO_3 868 cm^{-1} microwindow for the intercomparison period during

Nov. 11, 1996, pm.

Figure 15. Column results from NCAR SFIT analysis and JPL GGG analysis of spectra from JPL, NCAR and NPL in the HCl 2925.9 cm^{-1} microwindow for the intercomparison period during Nov. 11, 1996, pm.

Figure 16. Column results from NCAR SFIT analysis and JPL GGG analysis of spectra from JPL, NCAR and NPL in the O_3 3045.2 cm^{-1} microwindow for the intercomparison period during Nov. 11, 1996, pm.

Figure 17. Column results from NCAR SFIT analysis and JPL GGG analysis of spectra from JPL, NCAR and NPL in the HF 4039 cm^{-1} microwindow for the intercomparison period during Nov. 11, 1996, pm.

Table 1-1
Groups and Instruments Participating in the NDSC TMF Intercomparisons, Nov. 1996

Institute	Instrument	Code
JPL	ATMOS	GGG
JPL	MkIV	GGG
NCAR	Bruker 120M	SFIT
NPL	Bruker 120M	SFIT

Table 4-1
Initial Microwindows for the Blind Intercomparison, NDSC TMF, Nov. 1996

Molecule	Microwindow (cm^{-1})
HCl (& CH_4)	2925.80 - 2926.00
HF (& H_2O)	4038.78 - 4039.10
HNO_3	867.00 - 869.20
N_2O	2481.20 - 2482.50
O_3	3045.08 - 3045.38
N_2	2403.26 - 2403.86
CH_4 (& HCl, H_2O, HDO)	2903.50 - 2904.20

Table 4-2
Microwindows and Species used for the Blind Intercomparison, NDSC TMF, Nov. 1996

Molec.		Nominal Fit Region (cm^{-1})	Other Gases Included C-Const(fixed) F-Fitted
HF*	JPL	4038.78-4039.10	H_2O (F)
	NCAR	4038.78-4039.10	H_2O (F)
	NPL	4038.78-4039.10	H_2O (F)
HCl*	JPL	2925.80-2926.00	CH_4 (F)
	NCAR	2925.80-2926.00	CH_4 (F)
	NPL	2925.80-2926.00	CH_4 (F)
O_3*	JPL	3045.08-3045.38	
	NCAR	3045.08-3045.38	
	NPL	3045.08-3045.38	
O_3	JPL	3027.44-3027.60	
	NCAR	3027.42-3027.60	
	NPL	3027.42-3027.60	
CH_4*	JPL	2903.50-2904.20	H_2O(F), HCl(F), HDO(F)
	NCAR	2903.50-2904.20	H_2O(F), HCl(F), HDO(F)
	NPL	2903.50-2904.20	H_2O(F), HCl(F)
N_2	JPL	2418.40-2418.90	N_2O(C)
	NCAR	2418.40-2418.90	
	NPL	2418.40-2418.90	
N_2*	JPL	2403.26-2403.86	
	NCAR	2403.26-2403.86	
	NPL	2403.26-2403.86	
N_2	JPL	2410.86-2411.64	H_2O(F)
	NCAR	2410.86-2411.64	H_2O(F)
	NPL	2410.86-2411.64	H_2O(F)
N_2O*	JPL	2481.20-2482.50	
	NCAR	2481.20-2482.50	
	NPL	2481.20-2482.50	
N_2O	JPL	2441.80-2444.40	CO_2(F)
	NCAR	2441.80-2444.40	
	NPL	2441.80-2444.40	
HNO_3*	JPL	867.00-869.20	OCS(F)
	NCAR	867.00-869.20	
	NPL	867.00-869.20	
HNO_3	JPL	871.80-875.80	H_2O(F)
	NCAR	871.80-875.80	H_2O(F)
	NPL	871.80-875.80	
CO_2	JPL	936.44-937.18	
	NCAR	936.44-937.18	
	NPL	936.44-937.18	

*Initial microwindows.

Table 6-1
Summary of Column Measurements from the Blind Intercomparison, NDSC TMF, Nov. 11, 1996A

Molec. cm^{-1}	Solar Zenith Angle Range	No. of Obs	Mean Vertical Column (molecules cm^{-2})	Std. Dev. of Mean Column %	Average Column (molecules cm^{-2})	Percent from Average
N_2	JPL 53.245	6	1.304 E25	0.8		-0.8
2403	NCAR 53.9-52.7	8	1.311 E25	1.8	1.315 E25	-0.3
	NPL 54.0-52.7	16	1.33 E25	0.8		+1.1
N_2	JPL 53.245	6	1.291 E25	1.6		-1.0
2411	NCAR 53.9-52.7	8	1.290 E25	5.8	1.304 E25	-1.0
	NPL 54.0-52.7	16	1.33 E25	1.5		+2.0
N_2	JPL 53.245	6	1.357 E25	1.2		-0.1
2418	NCAR 53.9-52.7	8	1.351 E25	2.6	1.359 E25	-0.6
	NPL 54.0-52.7	16	1.37 E25	0.7		+0.8
HF	JPL 55.701	5	9.421 E14	0.96		-2.8
4039	NCAR 56.1-54.6	12	9.945 E14	2.3	9.695 E14	+2.6
	NPL 56.6-54.3	19	9.72 E14	0.4		+0.3
HCl	JPL 61.219	6	3.149 E15	1.7		-1.0
2926	NCAR 62.3-60.5	4	3.204 E15	2.3	3.181 E15	+0.7
	NPL 62.3-58.5	16	3.19 E15	0.9		+0.3
CH_4	JPL 61.219	6	2.738 E19	0.6		+0.9
2904	NCAR 62.3-59.4	8	2.653 E19	2.7	2.714 E19	-2.2
	NPL 62.3-58.5	16	2.75 E19	0.4		+1.3
O_3	JPL 61.219	6	6.748 E18	1.5		-1.3
3027	NCAR 62.3-59.4	8	6.847 E18	3.5	6.835 E18	+0.2
	NPL 62.3-58.5	16	6.91 E18	0.7		+1.1
O_3	JPL 61.219	6	6.869 E18	2.0		+1.0
3045	NCAR 62.3-59.4	8	6.619 E18	3.6	6.799 E18	-2.6
	NPL 62.3-58.5	16	6.91 E18	1.3		+1.6
N_2O	JPL 53.245	6	4.885 E18	0.6		-0.4
2442	NCAR 53.9-52.7	8	4.884 E18	1.3	4.903 E18	-0.4
	NPL 54.0-52.7	16	4.94 E18	0.2		+0.8
N_2O	JPL 53.245	6	4.930 E18	0.6		-0.7
2482	NCAR 53.9-52.7	8	4.938 E18	1.3	4.966 E18	-0.6
	NPL 54.0-52.7	16	5.03 E18	0.2		+1.3
HNO_3	JPL 68.315	6	1.047 E16	1.05		+5.2
868	NCAR 70.2-64.4	12	1.004 E16	5.3	9.957 E15	+0.8
	NPL 70.2-64.0	24	9.36 E15	0.9		-6.0
HNO_3	JPL 68.315	6	1.073 E16	1.8		+8.9
873	NCAR 70.2-64.4	12	9.287 E15	3.2	9.856 E15	-5.8
	NPL 70.2-64.0	24	9.55 E15	0.8		-3.1
CO_2	JPL 68.315	6	6.126 E21	1.4		+2.7
936	NCAR 70.2-64.4	12	5.763 E21	2.0	5.963 E21	-3.4
	NPL 70.2-64.0	24	6.00 E21	0.5		+0.6

Table 6-2
Summary of Column Measurements from the Blind Intercomparison, NDSC TMF, Nov. 11, 1996B

Molec. cm^{-1}	Solar Zenith Angle Range	No. of Obs	Mean Vertical Column (molecules cm^{-2})	Std. Dev. of Mean Column %	Average Column (molecules cm^{-2})	Percent from Average
N_2	JPL 54.792	6	1.292 E25	1.0		-1.7
2403	NCAR 54.1-55.8	14	1.331 E25	0.5	1.314 E25	+1.3
	NPL 54.1-56.0	10	1.32 E25	1.5		+0.5
N_2	JPL 54.792	6	1.291 E25	2.0		-1.7
2411	NCAR 54.1-55.8	14	1.337 E25	1.7	1.313 E25	+1.8
	NPL 54.1-56.0	10	1.31 E25	1.5		-0.2
N_2	JPL 54.792	6	1.346 E25	1.3		-0.7
2418	NCAR 54.1-55.8	14	1.358 E25	0.8	1.355 E25	+0.2
	NPL 54.1-56.0	10	1.36 E25	1.5		+0.4
HF	JPL 53.358	6	9.474 E14	1.1		-2.9
4039	NCAR 52.9-53.8	14	9.965 E14	0.6	9.760 E14	+2.1
	NPL 52.9-53.9	16	9.84 E14	0.5		+0.8
HCl	JPL 52.103	6	3.112 E15	1.7		-1.6
2926	NCAR 52.0-52.6	22	3.189 E15	0.9	3.164 E15	+0.8
	NPL 52.0-52.6	16	3.19 E15	0.9		+0.8
CH_4	JPL 52.103	6	2.727 E19	0.6		-0.2
2904	NCAR 52.0-52.6	22	2.731 E19	0.7	2.733 E19	-0.1
	NPL 52.2-52.6	16	2.74 E19	0.4		+0.3
O_3	JPL 52.101	6	6.695 E18	1.4		-2.0
3027	NCAR 52.0-52.6	22	6.954 E18	0.9	6.833 E18	+1.8
	NPL 52.2-52.6	16	6.85 E18	0.7		+0.2
O_3	JPL 52.101	6	6.770 E18	1.7		-0.4
3045	NCAR 52.0-52.6	22	6.742 E18	2.3	6.794 E18	-0.8
	NPL 52.2-52.5	16	6.87 E18	1.7		+1.1
N_2O	JPL 54.792	6	4.903 E18	0.7		-0.2
2442	NCAR 54.1-55.8	14	4.922 E18	0.2	4.912 E18	+0.2
	NPL 54.1-56.0	10	4.91 E18	0.2		0.0
N_2O	JPL 54.792	6	4.944 E18	0.6		-0.6
2482	NCAR 54.1-55.8	14	4.963 E18	0.2	4.972 E18	-0.2
	NPL 54.1-56.0	16	5.01 E18	0.2		+0.8
HNO_3	JPL 58.200	6	9.837 E15	1.4		+2.2
868	NCAR 56.7-58.9	14	9.654 E15	1.5	9.627 E15	+0.3
	NPL 56.6-59.4	14	9.39 E15	1.0		-2.5
HNO_3	JPL 58.200	6	9.908 E15	2.5		+4.1
873	NCAR 56.7-58.9	14	9.276 E15	2.0	9.518 E15	-2.5
	NPL 56.6-59.4	14	9.37 E15	1.5		-1.6
CO_2	JPL 58.200	6	6.089 E21	1.2		+1.6
936	NCAR 56.7-58.9	14	5.868 E21	0.25	5.996 E21	-2.1
	NPL 56.6-59.4	14	6.03 E21	0.3		+0.6

Table 6-3
Summary of Column Measurements from the Blind Intercomparison, NDSC TMF, Nov. 15, 1996

Molec. cm^{-1}	Solar Zenith Angle Range	No. of Obs	Mean Vertical Column (molecules cm^{-2})	Std. Dev. of Mean Column %	Average Column (molecules cm^{-2})	Percent From Average
N_2	JPL 66.602	3	1.276 E25	2.1		-1.2
2403	NCAR 67.2-65.5	7	1.306 E25	2.9	1.291 E25	+1.2
	NPL 67.2-65.2	10	1.29 E25	5.4		-0.1
N_2	JPL 66.602	3	1.346 E25	3.3		+0.4
2411	NCAR 67.2-65.5	7	1.363 E25	3.5	1.340 E25	+1.7
	NPL 67.2-65.2	10	1.31 E25	5.3		-2.2
N_2	JPL 66.602	3	1.359 E25	1.8		+2.0
2418	NCAR 67.2-65.5	7	1.326 E25	4.4	1.332 E21	-0.5
	NPL 67.2-65.2	10	1.31 E25	6.1		-1.7
HF	JPL 69.700	4	1.059 E15	1.2		-2.2
4039	NCAR 70.5-68.0	8	1.089 E15	1.0	1.083 E15	+0.6
	NPL 70.5-68.9	9	1.10 E15	2.7		+1.6
HCl	JPL 71.656	4	3.593 E15	1.7		+1.4
2926	NCAR 73.6-71.5	6	3.496 E15	1.3	3.543 E15	-1.3
	NPL 75.2-70.9	10	3.54 E15	1.1		-0.1
CH_4	JPL 71.656	4	2.690 E19	0.9		+0.3
2904	NCAR 73.6-71.5	6	2.655 E19	1.0	2.682 E19	-1.0
	NPL 75.2-70.9	10	2.70 E19	0.7		+0.7
O_3	JPL 71.656	4	6.713 E18	2.2		+0.7
3027	NCAR 76.0-71.5	10	6.606 E18	1.1	6.666 E18	-0.9
	NPL 75.2-70.9	10	6.68 E18	1.8		+0.2
O_3	JPL 71.656	4	6.819 E18	2.2		+2.5
3045	NCAR 76.0-71.5	10	6.517 E18	0.9	6.655 E18	-2.1
	NPL 75.2-70.9	10	6.63 E18	1.8		-0.4
N_2O	JPL 66.602	3	4.813 E18	0.7		+0.7
2442	NCAR 67.2-65.5	7	4.786 E18	1.6	4.780 E18	+0.1
	NPL 67.2-65.2	10	4.74 E18	3.0		-0.8
N_2O	JPL 66.602	3	4.876 E18	0.7		+0.8
2482	NCAR 67.2-65.5	7	4.819 E18	1.4	4.838 E18	-0.4
	NPL 67.2-65.2	10	4.82 E18	3.1		-0.4
HNO_3	JPL 66.602	3	1.262 E16	1.1		+8.0
868	NCAR 64.4-62.1	11	1.112 E16	2.7	1.168 E16	-4.8
	NPL 64.3-62.1	11	1.13 E16	2.6		-3.3
HNO_3	JPL 66.602	3	1.275 E16	2.0		+8.1
873	NCAR 64.4-62.1	11	1.113 E16	3.5	1.179 E16	-5.6
	NPL 64.3-62.1	11	1.15 E16	4.3		+2.5
CO_2	JPL 66.602	3	5.249 E21	1.6		+1.1
936	NCAR 64.4-62.1	11	5.124 E21	0.9	5.194 E21	-1.3
	NPL 64.3-62.1	11	5.21 E21	1.3		+0.3

Table 6-4
Summary of the Column Measurements of Coadded Spectra from the Blind Intercomparison as used for the Spectral Plots in Figs. 1-7

Main Molecule		Solar Zenith Angle	Date	Nominal Microwindow (cm^{-1})	Coadded Spectra Column (molecules cm^{-2})
HNO_3	JPL	58.20	11.11.96B	867.00 - 869.20	9.695 E15
	NCAR	57.78	11.11.96B	867.00 - 869.20	9.244 E15
	NPL	65.22	11.11.96A	867.00 - 869.20	9.399 E15
N_2	JPL	53.25	11.11.96A	2418.40 - 2418.90	1.357 E25
	NCAR	54.95	11.11.96B	2418.40 - 2418.90	1.357 E25
	NPL	53.43	11.11.96A	2418.40 - 2418.90	1.374 E25
N_2O	JPL	54.79	11.11.96B	2481.20 - 2482.50	4.943 E18
	NCAR	54.95	11.11.96B	2481.20 - 2482.50	4.964 E18
	NPL	53.43	11.11.96A	2481.20 - 2482.50	5.031 E18
CH_4	JPL	52.48	11.11.96B	2903.50 - 2904.20	2.734 E19
	NCAR	52.06	11.11.96B	2903.50 - 2904.20	2.741 E19
	NPL	61.24	11.11.96A	2903.50 - 2904.20	2.748 E19
HCl	JPL	52.10	11.11.96B	2925.80 - 2926.00	3.183 E15
	NCAR	52.06	11.11.96B	2925.80 - 2926.00	3.198 E15
	NPL	61.24	11.11.96A	2925.80 - 2926.00	3.183 E15
O_3	JPL	52.10	11.11.96A	3045.08 - 3045.38	6.743 E18
	NCAR	52.06	11.11.96B	3045.08 - 3045.38	6.958 E18
	NPL	61.24	11.11.96A	3045.08 - 3045.38	6.908 E18
HF	JPL	53.36	11.11.96B	4038.78 - 4039.10	9.475 E14
	NCAR	53.35	11.11.96B	4038.78 - 4039.10	9.968 E14
	NPL	54.80	11.11.96A	4038.78 - 4039.10	9.742 E14

Table 8-1
Zero level corrections for the HNO_3 and CO_2 intervals, NCAR Post-Analysis

Date	HNO_3		CO_2
	868 cm^{-1}	873 cm^{-1}	937 cm^{-1}
961111A	3.4%	3.3%	2.3%
961111B	4.1%	4.0%	2.7%
961115	6.3%	6.1%	3.6%

Table 8-2
Zero level corrections for the HNO_3 and CO_2 intervals, NPL Post-Analysis

Date	HNO_3		CO_2
	868 cm^{-1}	873 cm^{-1}	937 cm^{-1}
961111A	3.9%	3.9%	2.3%
961111B	4.0%	4.0%	2.4%
961115	2.6%	2.6%	1.6%

Table 8-3
Summary of Column Measurements from the Post-Analysis, NDSC TMF, Nov. 11, 1996A

Molec. cm^{-1}	Solar Zenith Angle Range	No. of Obs	Mean Vertical Column (molecules cm^{-2})	Std. Dev. of Mean Column %	Average Column (molecules cm^{-2})	Percent from Average
N_2 2403	JPL 53.245	6	1.304 E25	1.0*	1.316 E25*	-0.9*
	NCAR 53.9-52.7	8	1.314 E25[x]	1.8		-0.2*
	NPL 54.0-52.7	16	1.33 E25	0.8		+1.1
N_2 2411	JPL 53.245	6	1.291 E25	1.6	1.304 E25	-1.0
	NCAR 53.9-52.7	8	1.290 E25	5.8		-1.0
	NPL 54.0-52.7	16	1.33 E25	1.5		+2.0
N_2 2418	JPL 53.245	6	1.357 E25	1.3*	1.359 E25	-0.2*
	NCAR 53.9-52.7	8	1.351 E25	2.6		-0.6
	NPL 54.0-52.7	16	1.37 E25	0.7		+0.8
HF 4039	JPL 55.701	5	9.423 E14[x]	1.0*	9.713 E14*	-3.0*
	NCAR 56.1-54.6	12	9.995 E14[x]	2.0		+2.9*
	NPL 56.6-54.3	19	9.72 E14	0.4		+0.1*
HCl 2926	JPL 61.219	6	3.160 E15[x]	1.6*	3.176 E15*	-0.5*
	NCAR 62.3-60.5	4	3.177 E15*	2.9		+0.03*
	NPL 62.3-58.5	16	3.19 E15	0.9		+0.5*
CH_4 2904	JPL 61.219	6	2.753 E19[x]	0.7*	2.727 E19*	+1.0*
	NCAR 62.3-59.4	8	2.677 E19*	1.8		-1.8*
	NPL 62.3-58.5	16	2.75 E19	0.4		+0.8*
O_3 3027	JPL 61.219	6	6.759 E18[x]	1.8*	6.839 E18	-1.2*
	NCAR 62.3-59.4	8	6.847 E18	3.5		+0.1*
	NPL 62.3-58.5	16	6.91 E18	0.7		+1.0*
O_3 3045	JPL 61.219	6	6.831 E18[x]	2.0	6.855 E18*	-0.4*
	NCAR 62.3-59.4	8	6.825 E18*	2.8*		-0.4*
	NPL 62.3-58.5	16	6.91 E18	1.3		+0.8*
N_2O 2442	JPL 53.245	6	4.886 E18[x]	1.0*	4.923 E18*	-0.8*
	NCAR 53.9-52.7	8	4.943 E18*	1.3		+0.4*
	NPL 54.0-52.7	16	4.94 E18	0.2		+0.4*
N_2O 2482	JPL 53.245	6	4.931 E18[x]	1.0*	4.948 E18*	-0.4*
	NCAR 53.9-52.7	8	4.884 E18*	1.3		-1.3*
	NPL 54.0-52.7	16	5.03 E18	0.2		+1.7*
HNO_3 868	JPL 68.315	6	1.023 E16*	0.9*	9.972 E15*	+2.6*
	NCAR 70.2-64.4	12	9.956 E15*	5.3		-0.2*
	NPL 70.2-64.0	24	9.73 E15*	0.8*		-2.4*
HNO_3 873	JPL 68.315	6	1.036 E16*	0.9*	9.967 E15*	+3.9*
	NCAR 70.2-64.4	12	9.602 E15*	3.2		-3.7*
	NPL 70.2-64.0	24	9.94 E15*	0.8		-0.3*
CO_2 936	JPL 68.315	6	6.123 E21[x]	0.7*	6.075 E21*	+0.8*
	NCAR 70.2-64.4	12	5.931 E21*	2.0		-2.4*
	NPL 70.2-64.0	24	6.17 E21*	0.5		+1.6*

*Revised from the blind intercomparison.
[x]Column changed by less than 0.5%.

Table 8-4
Summary of Column Measurements from the Post-Analysis, NDSC TMF, Nov. 11, 1996B

Molec. cm^{-1}	Solar Zenith Angle Range	No. of Obs	Mean Vertical Column (molecules cm^{-2})	Std. Dev. of Mean Column %	Average Column (molecules cm^{-2})	Percent from Average
N_2	JPL 54.792	6	1.291 E25[x]	1.1*		-1.8*
2403	NCAR 54.1-55.8	14	1.333 E25[x]	0.5	1.315 E25*	+1.4*
	NPL 54.1-56.0	10	1.32 E25	1.5		+0.4*
N_2	JPL 54.792	6	1.290 E25[x]	1.9*		-1.6*
2411	NCAR 54.1-55.8	14	1.334 E25[x]	1.3	1.311 E25*	+1.7*
	NPL 54.1-56.0	10	1.31 E25	1.5		-0.1*
N_2	JPL 54.792	6	1.346 E25	1.3		-0.7
2418	NCAR 54.1-55.8	14	1.358 E25	0.8	1.355 E25	+0.2
	NPL 54.1-56.0	10	1.36 E25	1.5		+0.4
HF	JPL 53.358	6	9.470 E14[x]	1.2*		-3.2*
4039	NCAR 52.9-53.8	14	1.004 E15*	0.6	9.783 E14*	+2.6*
	NPL 52.9-53.9	16	9.84 E14	0.5		+0.6*
HCl	JPL 52.103	6	3.114 E15[x]	1.6*		-1.6
2926	NCAR 52.0-52.6	22	3.190 E15[x]	0.9	3.165 E15	+0.8
	NPL 52.0-52.6	16	3.19 E15	0.9		+0.8
CH_4	JPL 52.103	6	2.733 E19[x]	0.6		-0.2*
2904	NCAR 52.0-52.6	22	2.744 E19[x]	0.8	2.739 E19*	+0.2*
	NPL 52.2-52.6	16	2.74 E19	0.4		+0.04*
O_3	JPL 52.101	6	6.757 E18[x]	1.6*		-1.4*
3027	NCAR 52.0-52.6	22	6.954 E18	0.9	6.854 E18	+1.4*
	NPL 52.2-52.6	16	6.85 E18	0.7		+0.06*
O_3	JPL 52.101	6	6.775 E18[x]	1.9*		-1.4*
3045	NCAR 52.0-52.6	22	6.981 E18*	0.9	6.875 E18*	+1.5*
	NPL 52.2-52.5	16	6.87 E18	1.7		-0.1*
N_2O	JPL 54.792	6	4.899 E18[x]	1.0*		-0.5*
2442	NCAR 54.1-55.8	14	4.968 E18*	0.2	4.926 E18*	+0.8*
	NPL 54.1-56.0	10	4.91 E18	0.2		-0.3*
N_2O	JPL 54.792	6	4.939 E18[x]	0.7*		-0.4*
2482	NCAR 54.1-55.8	14	4.922 E18*	0.2	4.957 E18*	-0.7*
	NPL 54.1-56.0	16	5.01 E18	0.2		+1.1*
HNO_3	JPL 58.200	6	9.885 E15[x]	1.0*		+1.0*
868	NCAR 56.7-58.9	14	9.632 E15[x]	1.4	9.782 E15*	-1.5*
	NPL 56.6-59.4	14	9.83 E15*	0.9*		+0.5*
HNO_3	JPL 58.200	6	1.000 E16*	1.1*		+2.1*
873	NCAR 56.7-58.9	14	9.655 E15*	2.0	9.795 E15*	-1.4*
	NPL 56.6-59.4	14	9.73 E15*	1.4*		-0.7*
CO_2	JPL 58.200	6	6.084 E21[x]	0.6*		-0.5*
936	NCAR 56.7-58.9	14	6.060 E21*	0.25	6.115 E21*	-0.9*
	NPL 56.6-59.4	14	6.20 E21*	0.3		+1.4*

*Revised from the blind intercomparison.
[x]Column changed by less than 0.5%.

Table 8-5
Summary of Column Measurements from the Post-Analysis, NDSC TMF, Nov. 15, 1996

Molec. cm^{-1}	Solar Zenith Angle Range	No. of Obs	Mean Vertical Column (molecules cm^{-2})	Std. Dev. of Mean Column %	Average Column (molecules cm^{-2})	Percent From Average
N_2	JPL 66.602	3	1.282 E25[x]	3.0*		-0.9*
2403	NCAR 67.2-65.5	7	1.309 E25[x]	2.9	1.294 E25*	+1.2*
	NPL 67.2-65.2	10	1.29 E25	5.4		-0.3*
N_2	JPL 66.602	3	1.351 E25[x]	3.9*		+2.0*
2411	NCAR 67.2-65.5	7	1.313 E25*	4.1*	1.325 E25*	-0.9*
	NPL 67.2-65.2	10	1.31 E25	5.3		-1.1*
N_2	JPL 66.602	3	1.363 E25[x]	2.6*		+2.2*
2418	NCAR 67.2-65.5	7	1.326 E25	4.4	1.333 E21	-0.5
	NPL 67.2-65.2	10	1.31 E25	6.1		-1.7
HF	JPL 69.700	4	1.063 E15[x]	1.2		-2.1*
4039	NCAR 70.5-68.0	8	1.093 E15[x]	0.9*	1.085 E15*	+0.7*
	NPL 70.5-68.9	9	1.10 E15	2.7		+1.4*
HCl	JPL 71.656	4	3.600 E15[x]	1.7		+1.5*
2926	NCAR 73.6-71.5	6	3.503 E15[x]	1.2*	3.548 E15*	-1.3*
	NPL 75.2-70.9	10	3.54 E15	1.1		-0.2*
CH_4	JPL 71.656	4	2.710 E19*	1.1*		+0.8*
2904	NCAR 73.6-71.5	6	2.652 E19[x]	1.0	2.687 E19*	-1.3*
	NPL 75.2-70.9	10	2.70 E19	0.7		+0.5*
O_3	JPL 71.656	4	6.719 E18[x]	2.4*		+0.8*
3027	NCAR 76.0-71.5	10	6.589 E18[x]	1.1*	6.663 E18*	-1.1*
	NPL 75.2-70.9	10	6.68 E18	1.8		+0.3*
O_3	JPL 71.656	4	6.759 E18*	2.4*		+1.5*
3045	NCAR 76.0-71.5	10	6.594 E18*	0.7*	6.661 E18*	-1.0*
	NPL 75.2-70.9	10	6.63 E18	1.8		-0.5*
N_2O	JPL 66.602	3	4.838 E18*	1.5*		+1.0*
2442	NCAR 67.2-65.5	7	4.786 E18	1.6	4.788 E18	-0.04*
	NPL 67.2-65.2	10	4.74 E18	3.0		-1.0*
N_2O	JPL 66.602	3	4.902 E18*	1.2*		+1.1*
2482	NCAR 67.2-65.5	7	4.827 E18[x]	1.4	4.850 E18*	-0.5*
	NPL 67.2-65.2	10	4.82 E18	3.1		-0.6*
HNO_3	JPL 66.602	3	1.229 E16*	1.1		+4.6*
868	NCAR 64.4-62.1	11	1.137 E16*	2.6*	1.175 E16*	-3.3*
	NPL 64.3-62.1	11	1.16 E16*	2.6		-1.3*
HNO_3	JPL 66.602	3	1.234 E16*	1.3*		+2.9*
873	NCAR 64.4-62.1	11	1.183 E16*	3.5	1.199 E16*	-1.3*
	NPL 64.3-62.1	11	1.18 E16*	5.1*		-1.6*
CO_2	JPL 66.602	3	5.248 E21[x]	1.0*		-1.0*
936	NCAR 64.4-62.1	11	5.346 E21*	0.9	5.301 E21*	+0.8*
	NPL 64.3-62.1	11	5.31 E21*	1.3		+0.2*

*Revised from the blind intercomparison.
[x]Column changed by less than 0.5%.

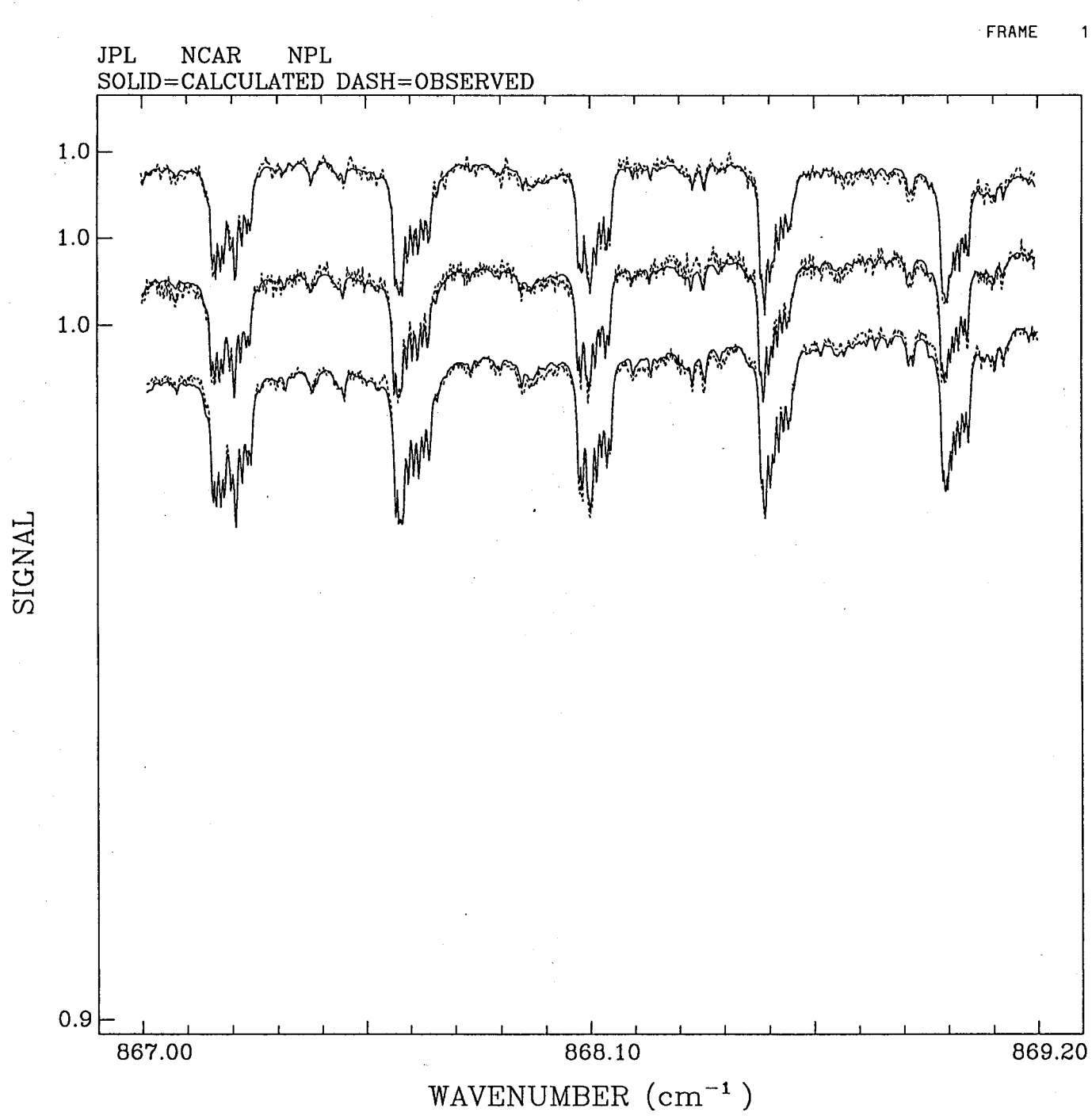
FRAME 1
HNO3
5/14/97
JPL NCAR NPL
SOLID=CALCULATED DASH=OBSERVED
1.0
1.0
1.0
0.9
SIGNAL
867.00
868.10
869.20
WAVENUMBER (cm⁻¹)

Fig. 1

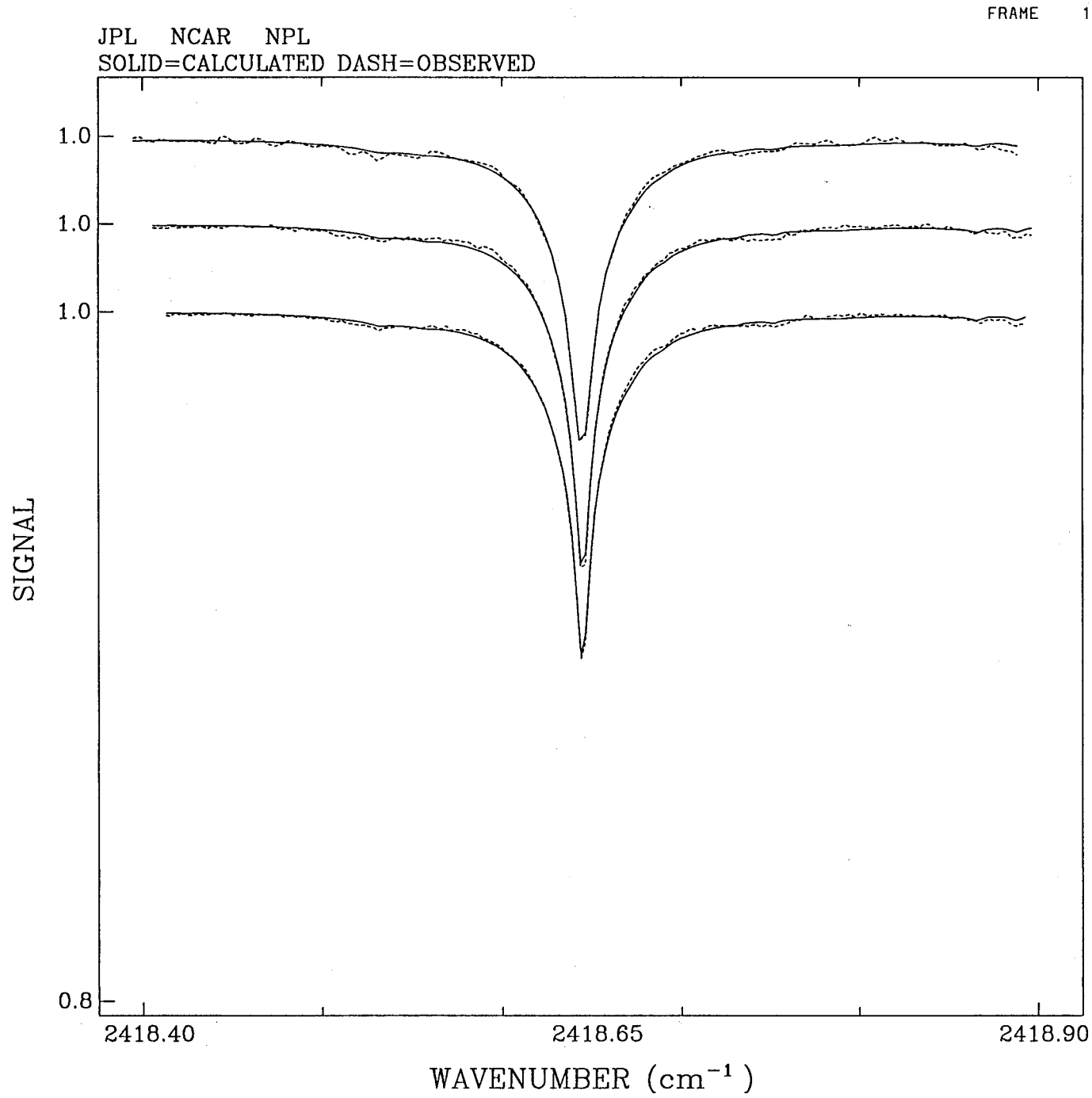

N_2
5/15/97

Fig. 2

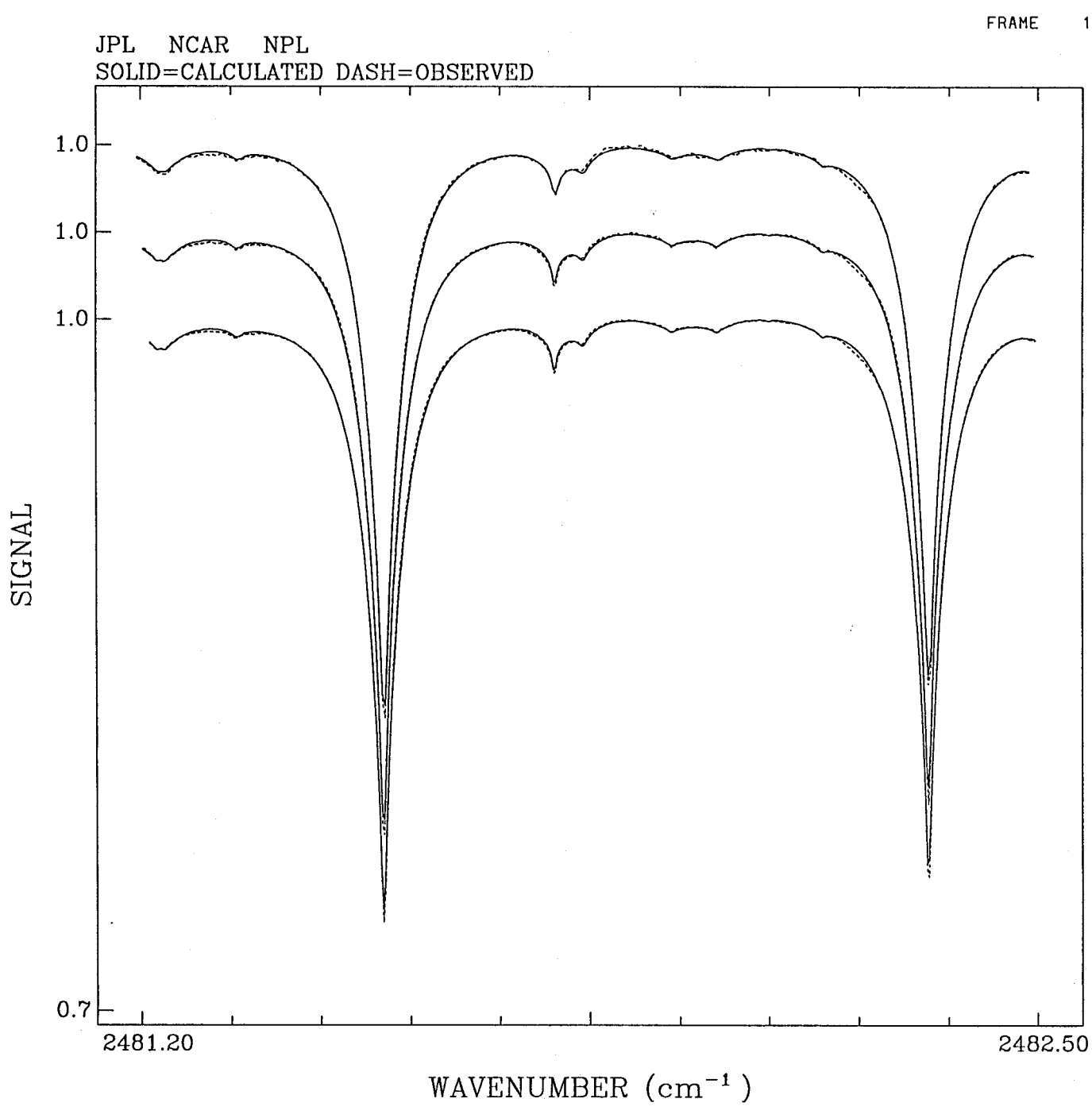

N_2O
5/16/97

Fig. 3

CH4
5/20/97

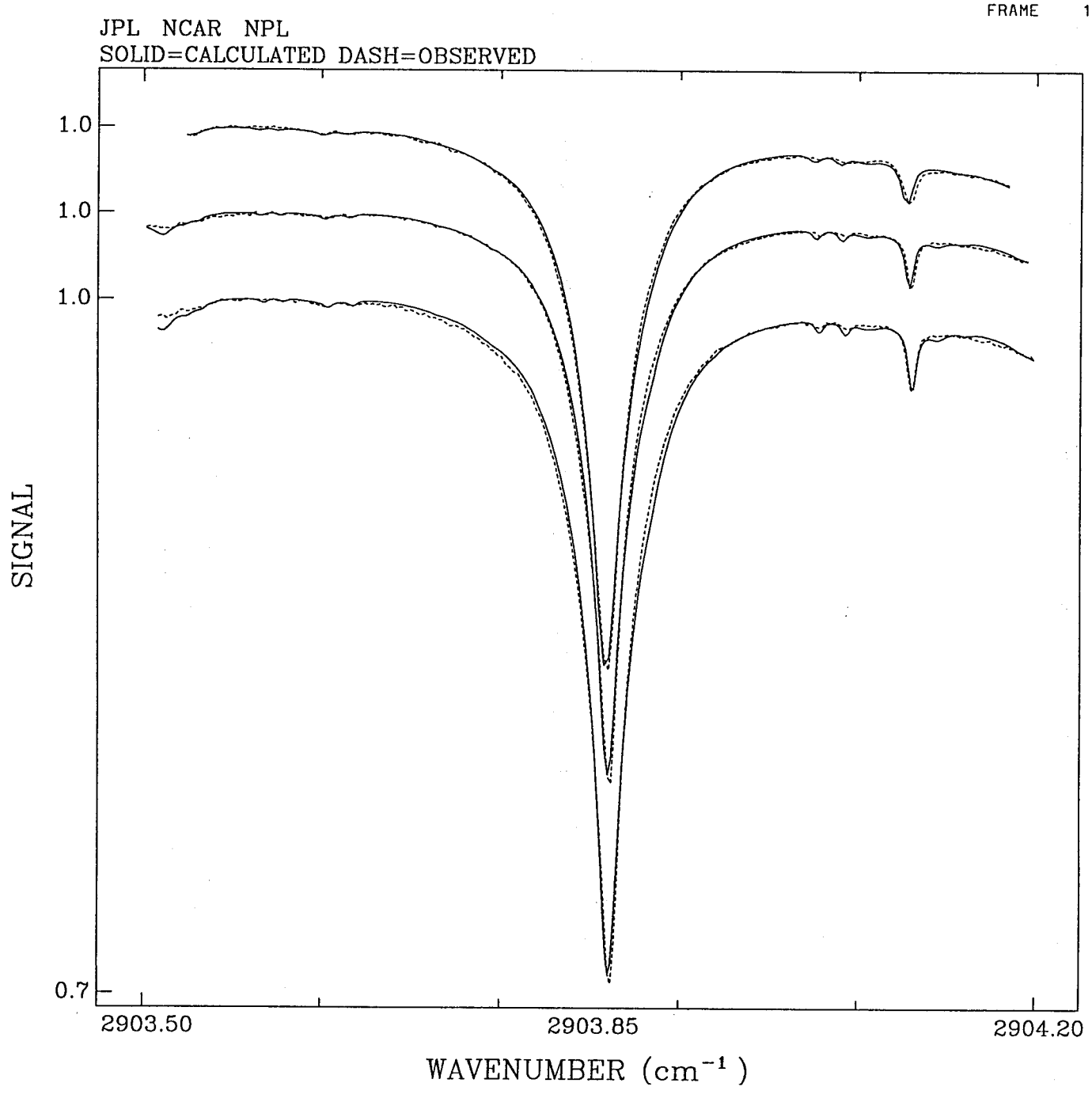

Fig. 4

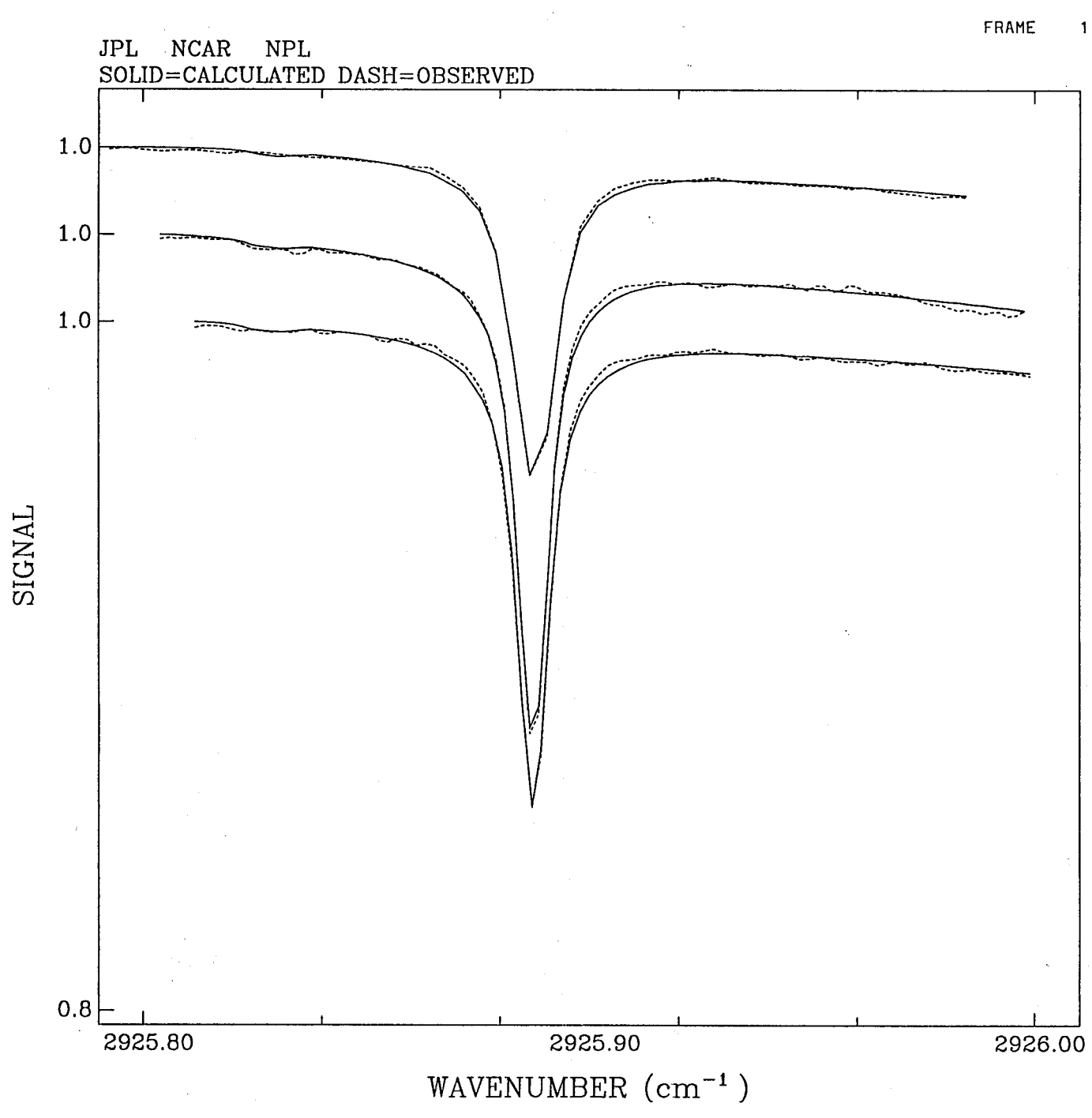

HCl
5/20/97

Fig. 5

03
5/20/97

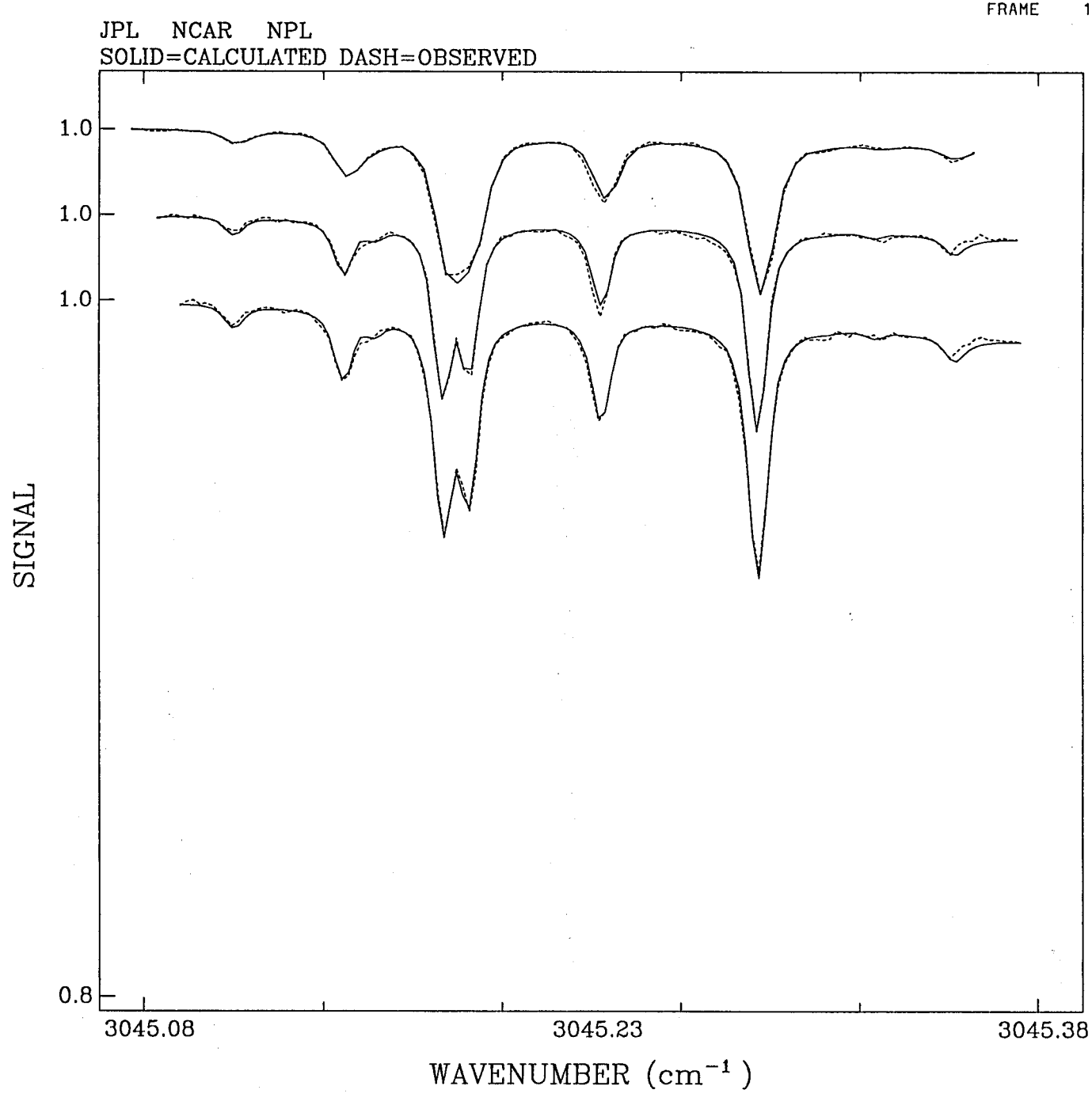

Fig. 6

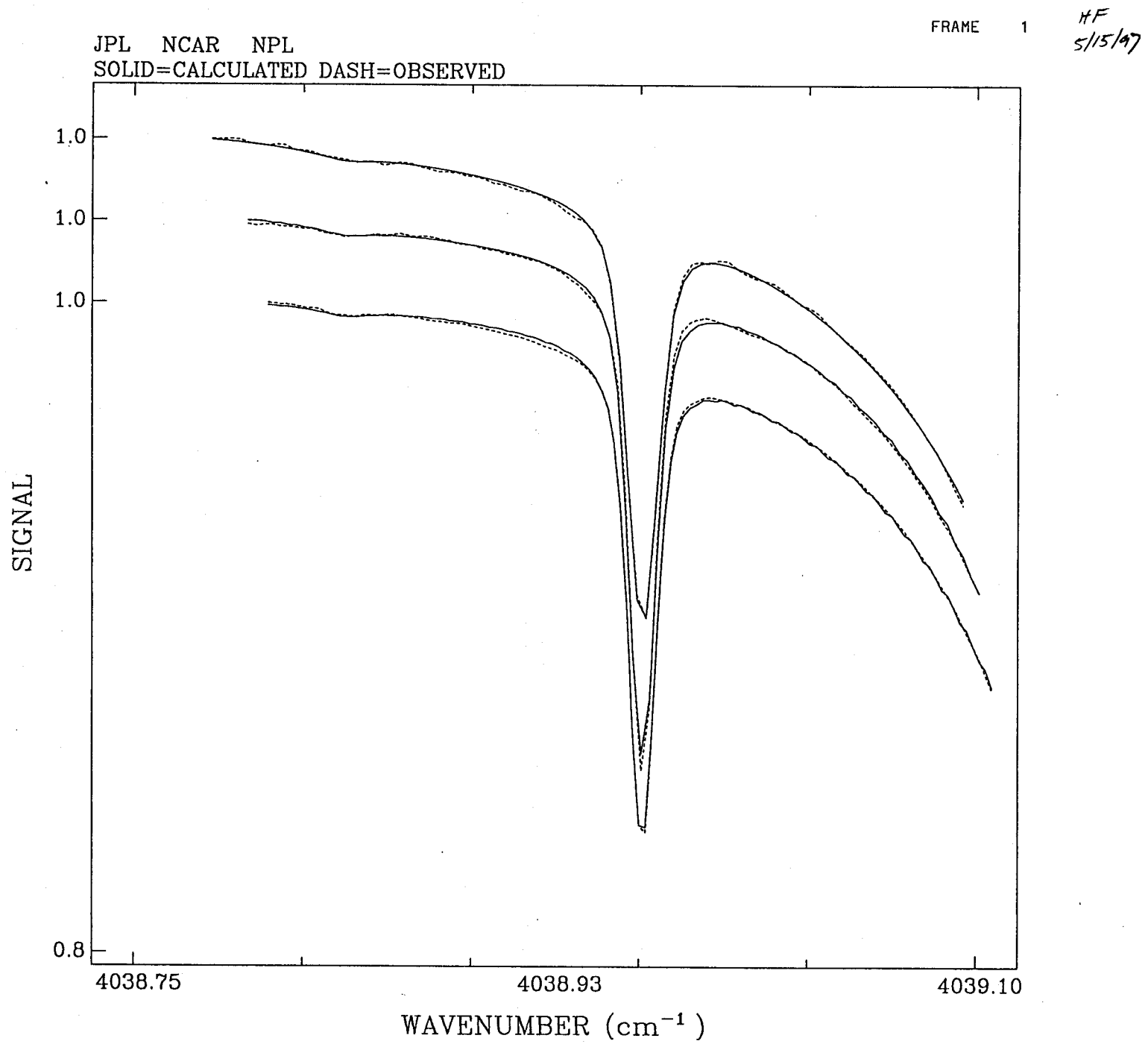

HF
5/15/97

Fig. 7

coffey 6/7/97

Mike will use these to create a new Fig. composite.

ID=05 SZA= 66.02 ONE-OPD=180.0 PROCESSED ON Sat Jun 7 06:17:59 1997
SPEC=D961116_2349-2550.005 ZPT=ZPTTMO41.NOV MX=REFTMO96.41
15/11/96 16:50:11 NSS 4 SST 35 OPD180 FOV3.864 SAN0 LLAE 34.4 117.7 2.24 23.98
EAPD=1.000 SD%=0.60

N20=4.9410E+018

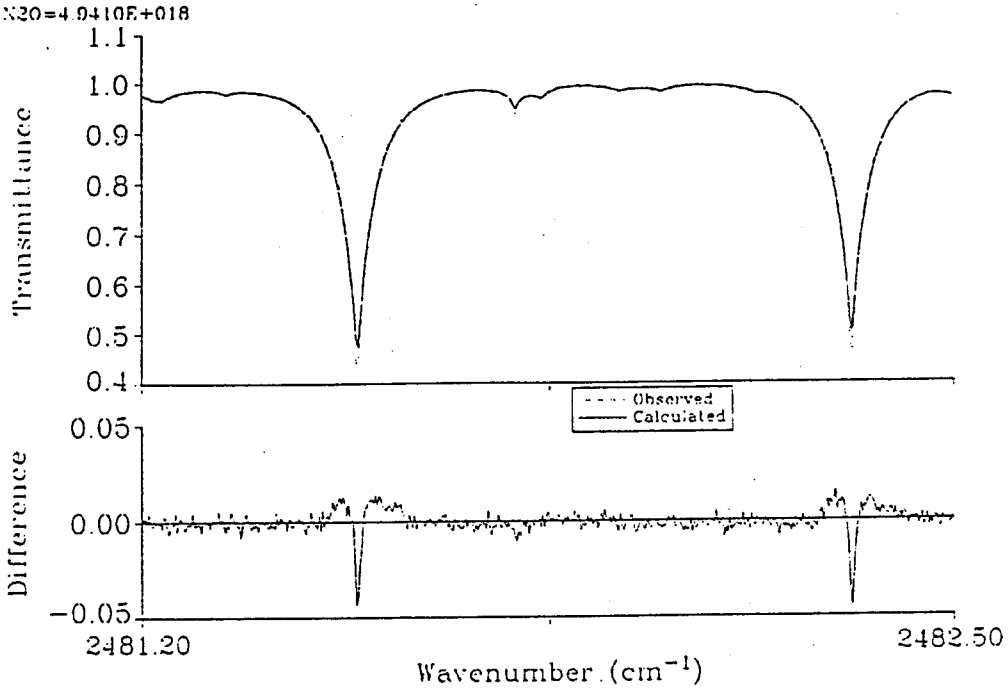

Fig 1 Top panel

ID=05 SZA= 66.02 ONE-OPD=180.0 PROCESSED ON Thu Sep 4 19:10:18 1997
SPEC=D961115_2349-2550.005 ZPT=ZPTTMO41.NOV MX=REFTMO96.41.ascN20
15/11/96 16:50:11 NSS 4 SST 35 OPD180 FOV3.864 SAN0 LLAE 34.4 117.7 2.24 23.98
EAPD=1.000 SD%=0.32

N20=4.8410E+018

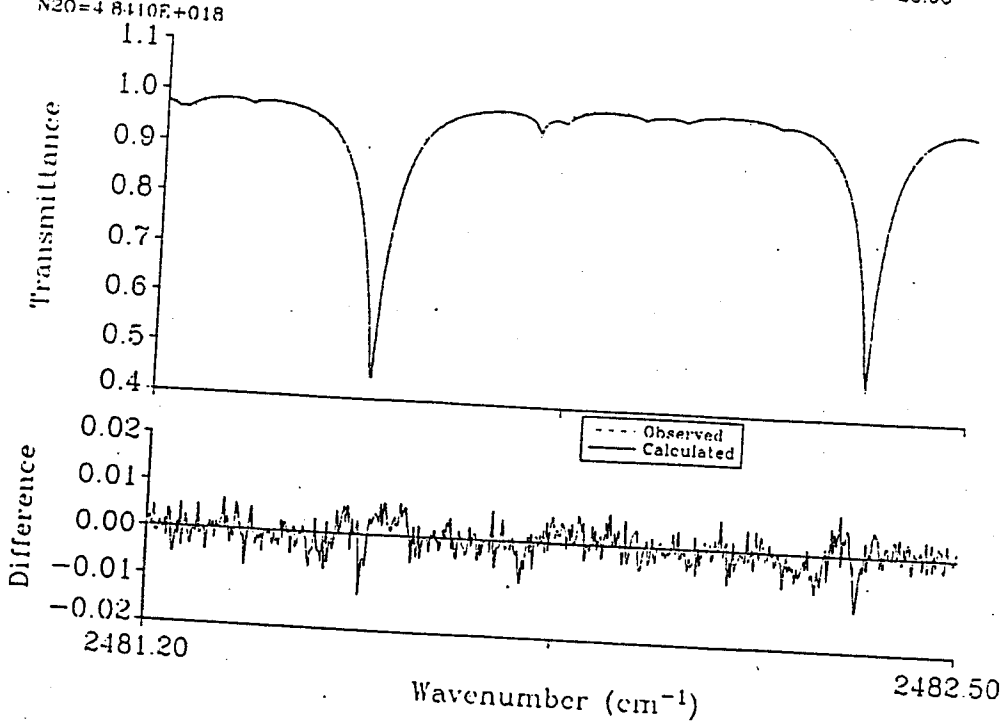

Fig 8

Fig 1 Bottom panel

CH4
5/21/97

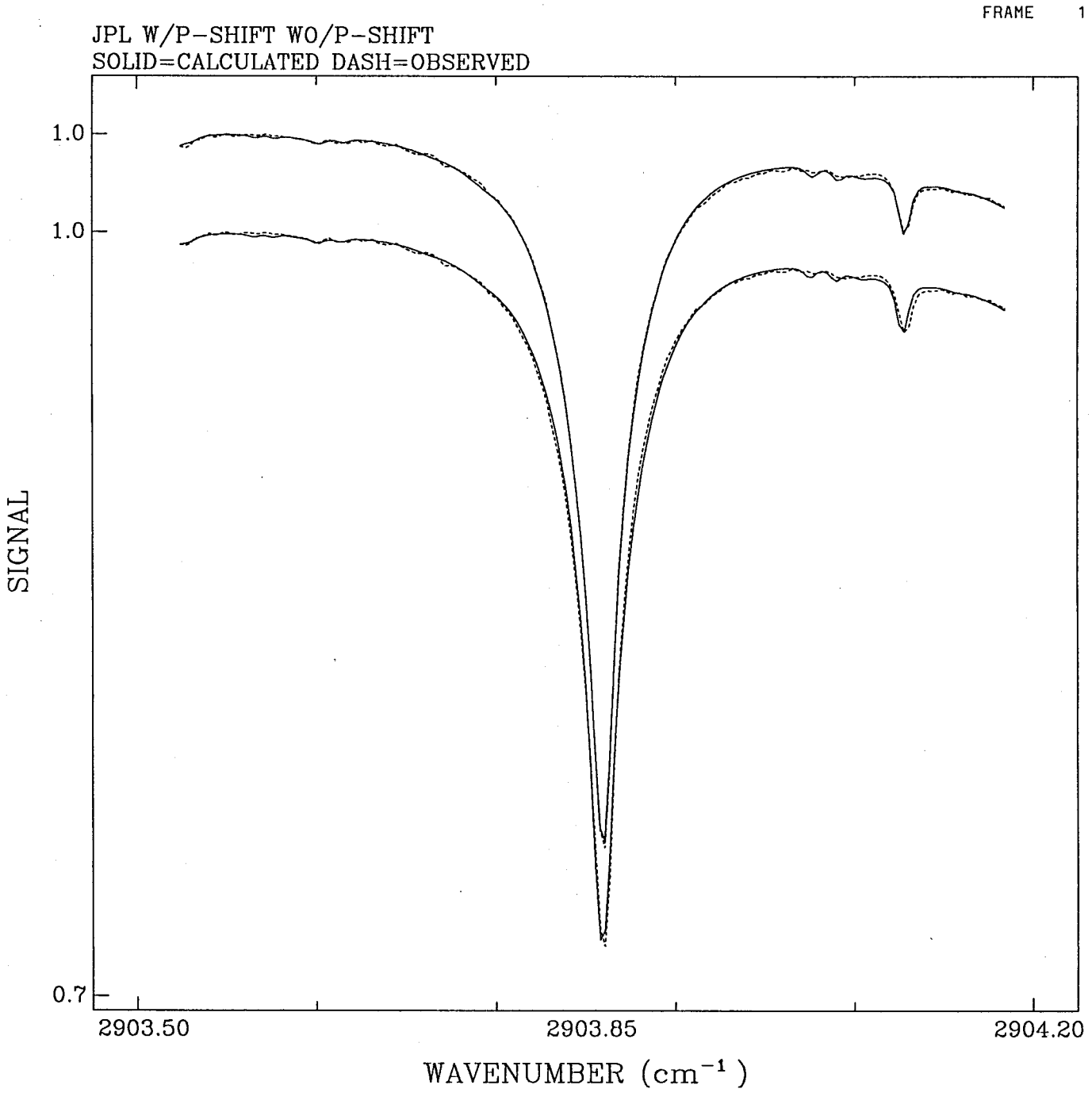

Fig. 9

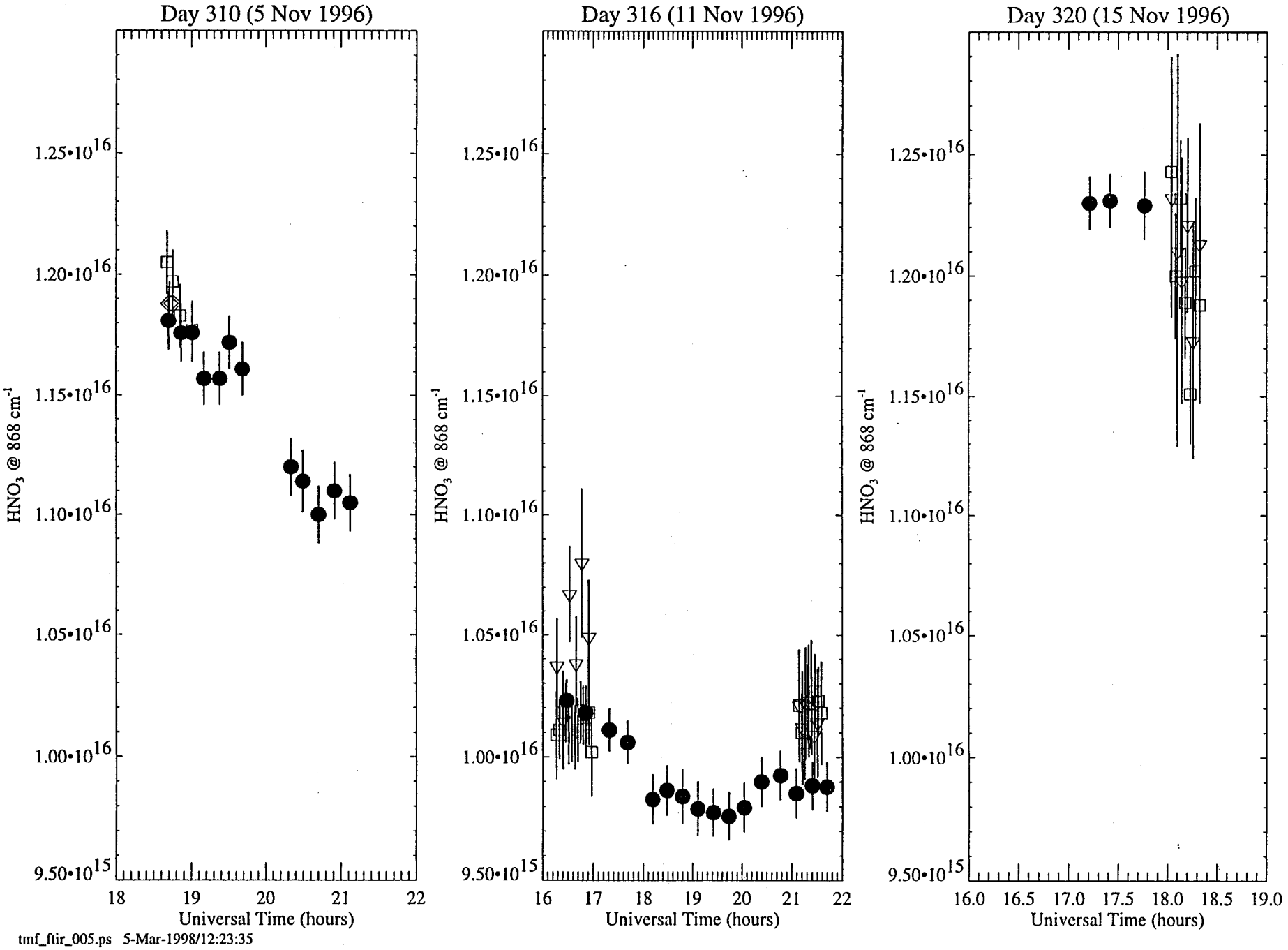
Day 310 (5 Nov 1996)
Day 316 (11 Nov 1996)
Day 320 (15 Nov 1996)
HNO_3 @ 868 cm^{-1}
1.25•10^16
1.20•10^16
1.15•10^16
1.10•10^16
1.05•10^16
1.00•10^16
9.50•10^15
18 19 20 21 22
16 17 18 19 20 21 22
16.0 16.5 17.0 17.5 18.0 18.5 19.0
Universal Time (hours)
tmf_ftir_005.ps 5-Mar-1998/12:23:35

Fig. 10

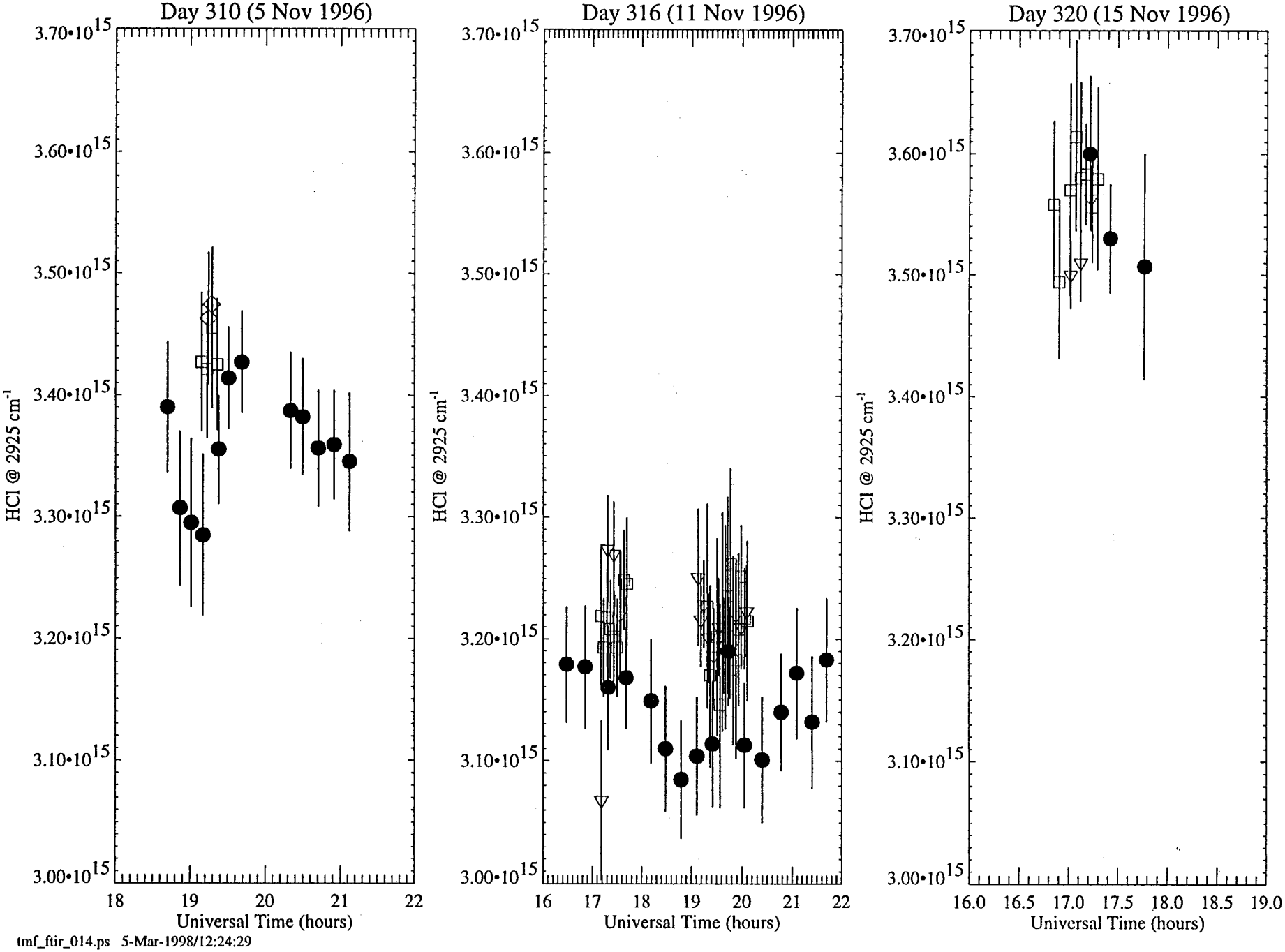
Day 310 (5 Nov 1996)
Day 316 (11 Nov 1996)
Day 320 (15 Nov 1996)
HCl @ 2925 cm-1
3.70•10^15
3.60•10^15
3.50•10^15
3.40•10^15
3.30•10^15
3.20•10^15
3.10•10^15
3.00•10^15
18
19
20
21
22
16
17
16.0
16.5
17.0
17.5
18.0
18.5
19.0
Universal Time (hours)
tmf_ftir_014.ps 5-Mar-1998/12:24:29

Fig. 11

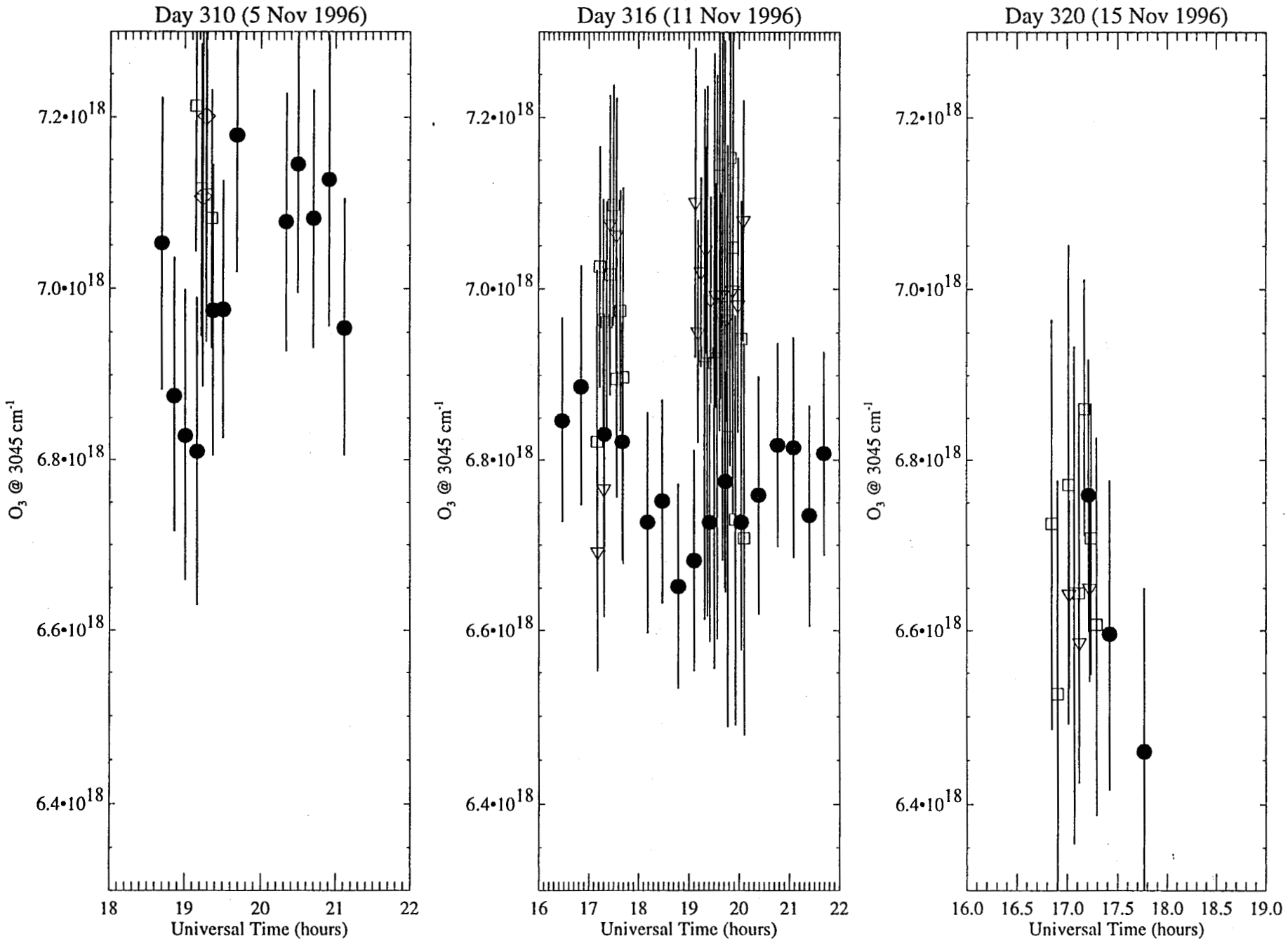
Day 310 (5 Nov 1996)
Day 316 (11 Nov 1996)
Day 320 (15 Nov 1996)
O_3 @ 3045 cm^{-1}
$7.2 \cdot 10^{18}$
$7.0 \cdot 10^{18}$
$6.8 \cdot 10^{18}$
$6.6 \cdot 10^{18}$
$6.4 \cdot 10^{18}$
18 19 20 21 22
16 17 18 19 20 21 22
16.0 16.5 17.0 17.5 18.0 18.5 19.0
Universal Time (hours)
tmf_ftir_016.ps 5-Mar-1998/12:24:40

Fig. 12

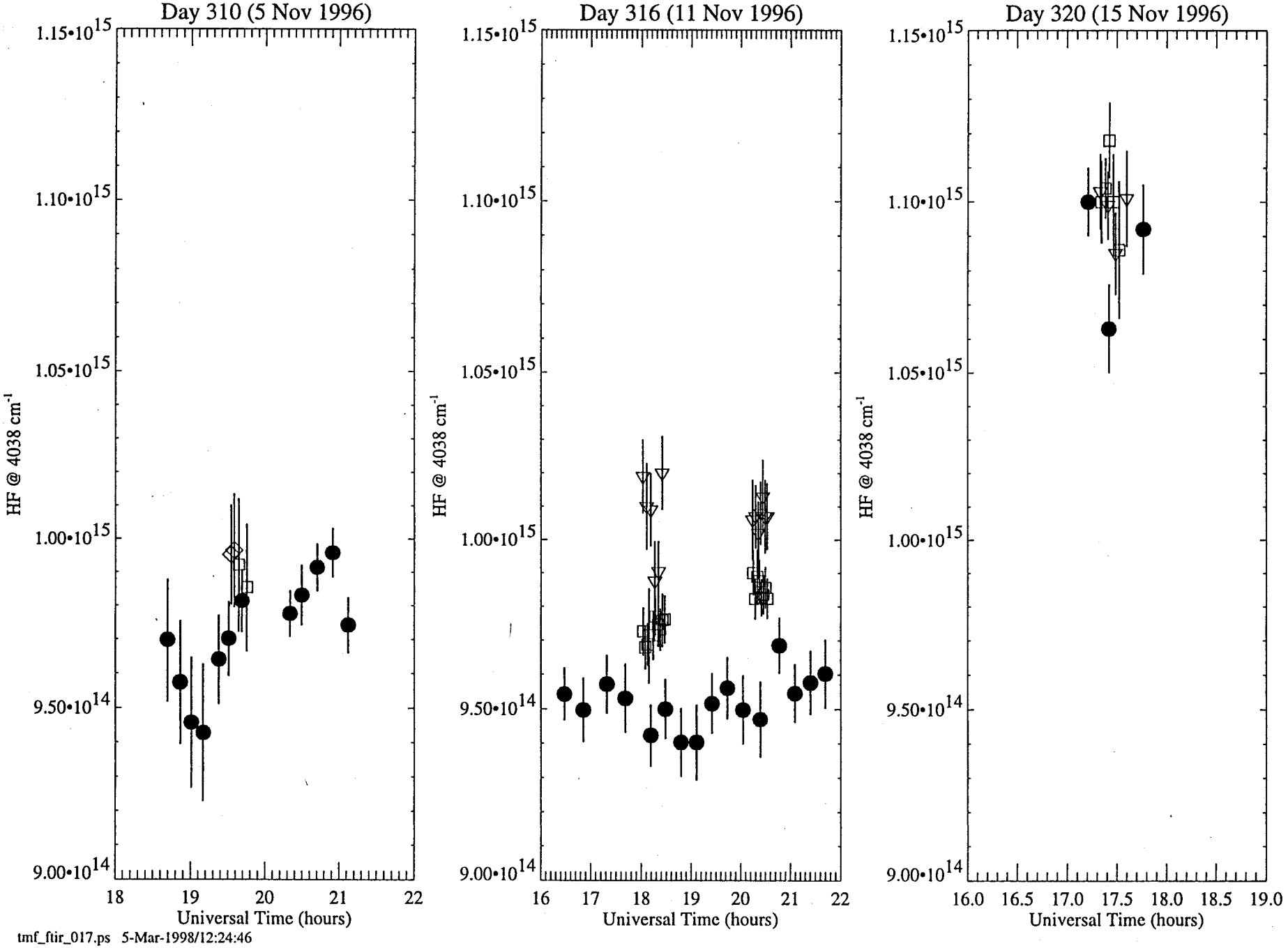
Day 310 (5 Nov 1996)
Day 316 (11 Nov 1996)
Day 320 (15 Nov 1996)
HF @ 4038 cm-1
1.15•10^15
1.10•10^15
1.05•10^15
1.00•10^15
9.50•10^14
9.00•10^14
18
19
20
21
22
16
17
16.0
16.5
17.0
17.5
18.0
18.5
19.0
Universal Time (hours)
tmf_ftir_017.ps 5-Mar-1998/12:24:46

Fig. 13

coffey
updated 3/4/99

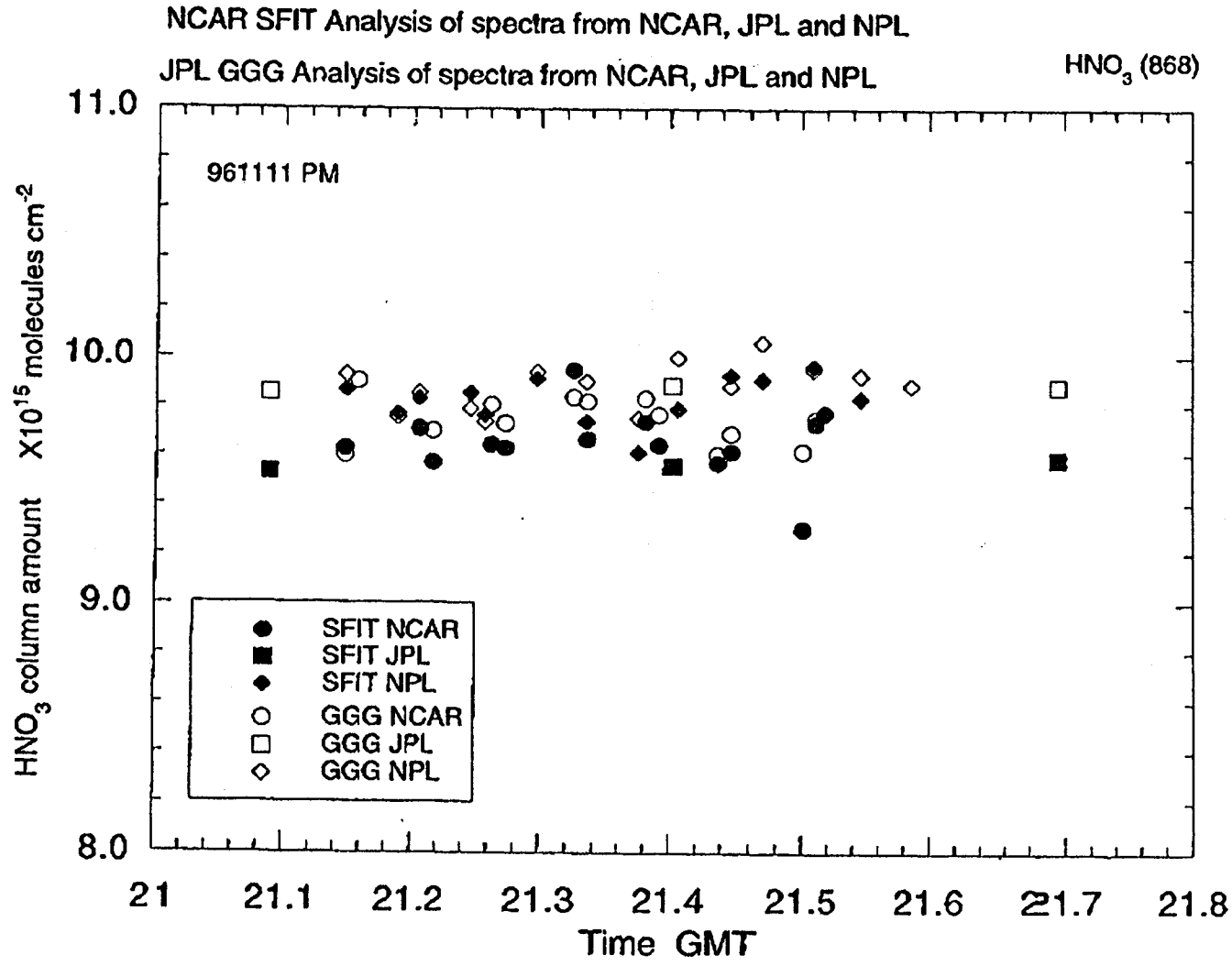

Fig. 14

coffey
updated 3/4/99

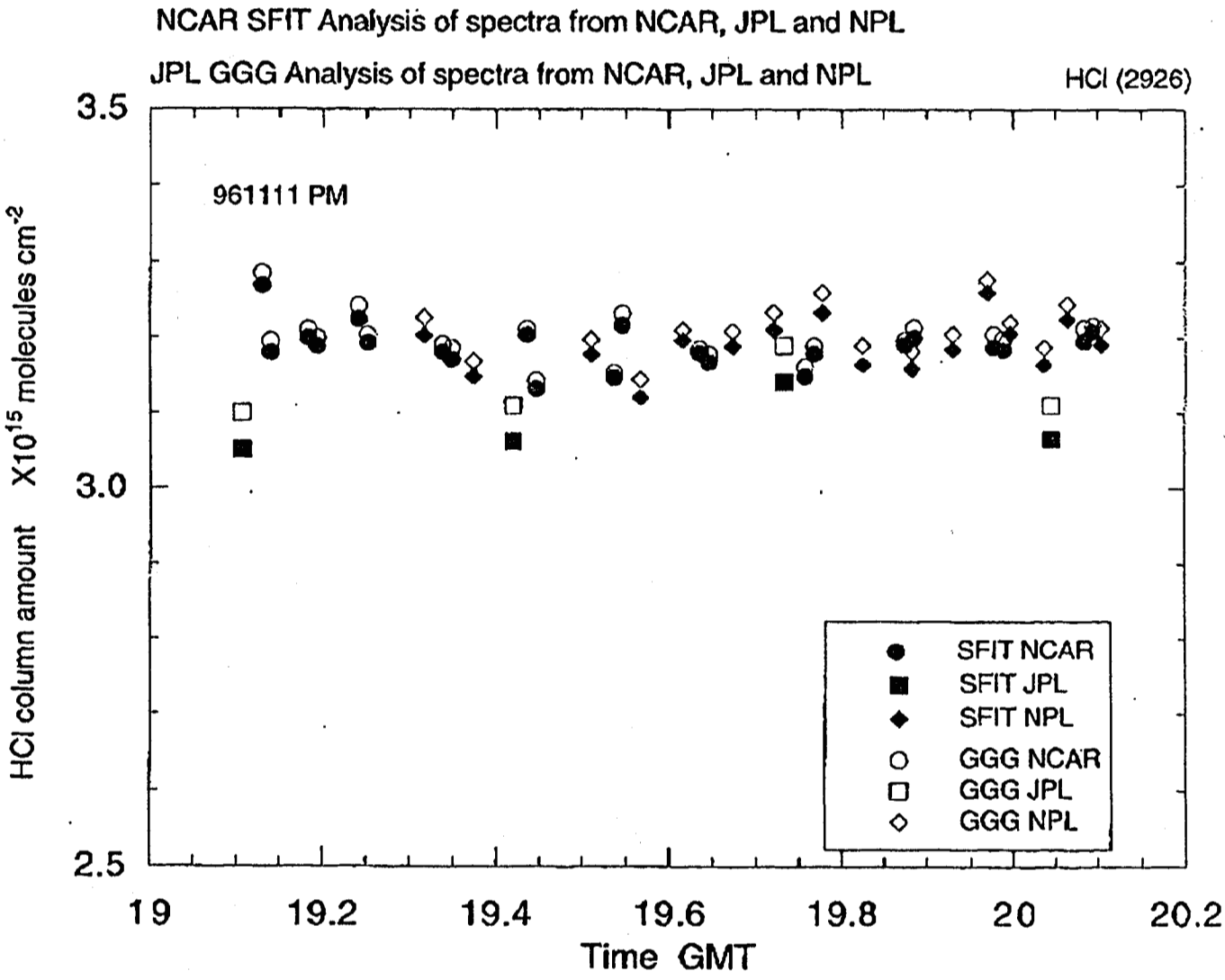

Fig. 15

coffey
updated 3/4/99

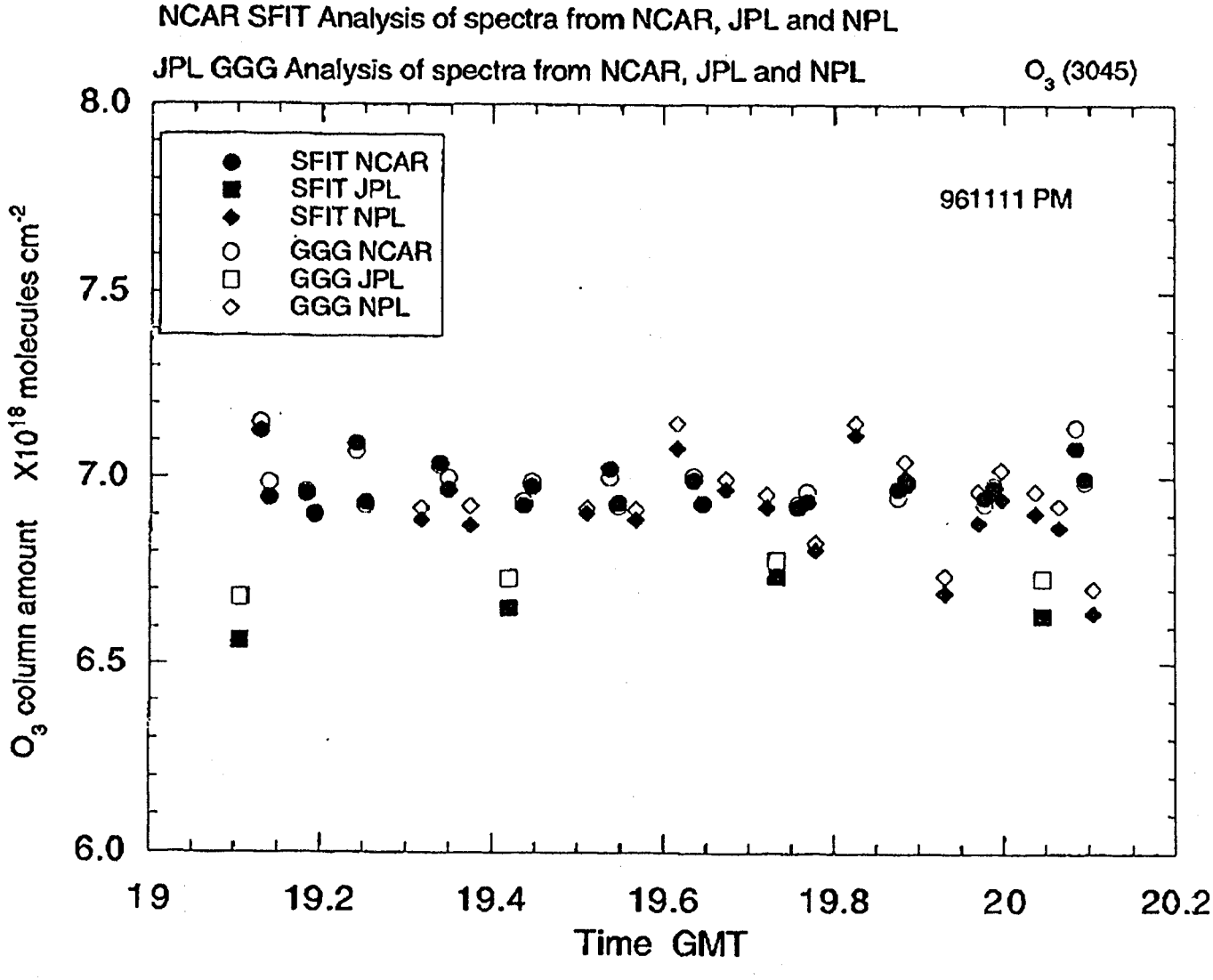

Fig. 16

coffey 4/16/99
with NPL SFIT HF added values. Will be replaced with NCAR SFIT HF values

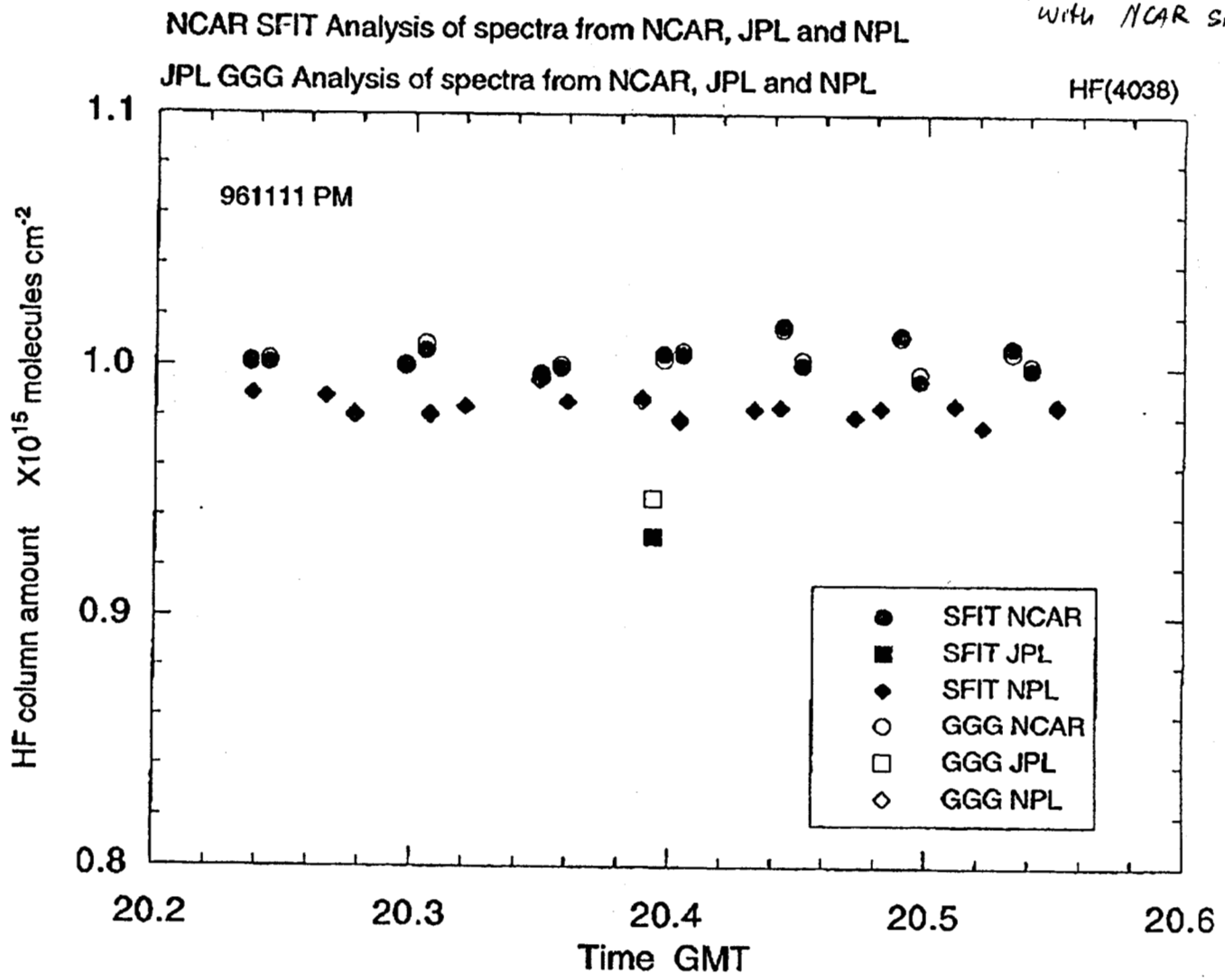

Fig. 17